

COUPLED DYNAMICS ANALYSIS
OF WIND ENERGY SYSTEMS

JOHN A. HOFFMAN

Paragon Pacific Incorporated

El Segundo, California

(NASA-CR-135152) COUPLED DYNAMICS ANALYSIS N77-20558
OF WIND ENERGY SYSTEMS Final Report
(Paragon Pacific, Inc., El Segundo, Calif.)
86 p HC A05/MF A01 CSCL 10A Unclass
G3/44 21740

prepared for

NATIONAL AERONAUTICS AND SPACE ADMINISTRATION

Lewis Research Center
Cleveland, Ohio

February 1977

Contract NAS 3-19767

REPRODUCED BY
NATIONAL TECHNICAL
INFORMATION SERVICE
U. S. DEPARTMENT OF COMMERCE
SPRINGFIELD, VA. 22161

1. Report No. NASA CR-135152		2. Government Accession No.		3. Recipient's Catalog No.	
4. Title and Subtitle COUPLED DYNAMICS ANALYSIS OF WIND ENERGY SYSTEMS				5. Report Date January 1977	
				6. Performing Organization Code	
7. Author(s) John A. Hoffman				8. Performing Organization Report No. PPI-1014-11	
9. Performing Organization Name and Address Paragon Pacific, Inc. 1601 E. El Segundo Blvd. El Segundo, California 90245				10. Work Unit No.	
				11. Contract or Grant No. NAS3-19767	
12. Sponsoring Agency Name and Address National Aeronautics and Space Administration Lewis Research Center Cleveland, Ohio				13. Type of Report and Period Covered Contractor Final Report	
				14. Sponsoring Agency Code	
15. Supplementary Notes					
16. Abstract <p>A qualitative description of all key elements of a complete wind energy system computer analysis code is presented. The analysis system addresses the coupled dynamics characteristics of wind energy systems, including the interactions of the rotor, tower, nacelle, power train, control system, and electrical network. The coupled dynamics are analyzed in both the frequency and time domains to provide the basic motions and loads data required for design, performance verification and operations analysis activities.</p> <p>Elements of the coupled analysis code were used to design and analyze candidate rotor articulation concepts for the NASA/ERDA Mod 0 Wind Turbine System. Fundamental results and conclusions derived from these studies are presented.</p> <p>The analysis results show that the teetering rotor develops approximately half the blade flap bending loads produced by a rigidly mounted hingeless rotor, using identical blades. Edgewise blade loads are approximately equal in the two systems.</p> <p>Flexibilities in the Mod 0 yaw drive, tower, nacelle and bearing mounts appear to be allowing the hingeless Mod 0 rotor to teeter to a substantial degree. Hence, the measured Mod 0 load levels are midway between calculated loads for the hingeless and teetering designs.</p> <p>Hingeless rotors with blade frequencies substantially below those of the current Mod 0 system develop lower flap bending loads at the expense of significantly higher edgewise bending loads. Such systems also require more blade/tower clearance to accommodate larger rotor coning excursions over the wind turbine system operational envelope.</p>					
17. Key Words (Suggested by Author(s)) Wind Energy Machines Windmills, Wind-Power Generators Windmill Dynamics, Wind Turbine Dynamics				18. Distribution Statement Unclassified - limited	
19. Security Classif. (of this report) Unclassified		20. Security Classif. (of this page) Unclassified			

* For sale by the National Technical Information Service, Springfield, Virginia 22161

FOREWORD

The work documented by this report was performed under Contract NAS 3-19767, issued by the NASA Lewis Research Center, Cleveland, Ohio 44135. The contract work was performed by Paragon Pacific, Inc., El Segundo, California 90245, under the direction of Mr. David C. Janetzke of NASA Lewis Research Center.

The author wishes to express sincere appreciation for the efforts of Mr. Janetzke in his support of the contractual work, which included guidance in designing and confirming the analytic computer codes and the assembly of fundamental input data for these analysis methods, as applicable to the NASA/ERDA Mod O Wind Turbine System.

TABLE OF CONTENTS

	Page
FOREWORD	iii
SUMMARY	1
INTRODUCTION	2
Evolution of the Wind Energy System Analysis Codes	2
Fundamental Objectives for the Coupled Dynamics Analysis Code	3
Design and Analysis of Candidate Mod-O Rotor Articulation Concepts	5
Organization of the Remaining Sections of this Report	5
OVERALL SYSTEM DESCRIPTION - WIND ENERGY SYSTEM COUPLED DYNAMICS ANALYSIS CODE	6
Overall System Arrangement	6
Subcode Data Interfaces	7
Sequence of Events - Coupled System Analysis	7
Fundamental Assumptions Incorporated in the Analysis	9
Alternative Analysis Methods	10
COMPONENT MODEL DESCRIPTIONS	12
Datain	12
Mostab-HFW	12
Rolim	14
The Coupled System Linear Analysis	14
DESIGN AND ANALYSIS OF CANDIDATE MOD O HUB ARTICULATION CONCEPTS	26
The Teetering System	26
The Elastic Interface Devices	27
General Conclusions - Articulation Devices	29
DISCUSSION OF RESULTS	29
CONCLUSIONS AND RECOMMENDATIONS FOR FURTHER RESEARCH	30
Verification of MOSTAS	30
Improved Accuracy	30

Select Nonlinearities	31
Utility Items	31
REFERENCES	32

TABLES:

I. History of MOSTAB/ROLIM Systems	33
II. Data Interfaces by Subcode; Wind Energy System Coupled Dynamics Analysis	34
III. Methods of Dynamic Analysis -- Rotor Systems	40
IV. Vectors for Wind Turbine Coupled System	41
V. Operators for Wind Turbine Coupled System	43
VI. Vector Lengths for Wind Turbine Coupled System	47
VII. Teetering Hub Design Concepts - Weights and Other Design Data	48
VIII. Blade Root Flexures - Summary	49

FIGURES:

1. Coupled Dynamics Analysis (MOSTAS) - Global Arrangements ...	50
2. Time and Frequency Domain Analysis Methods	51
3. Basic MOSTAB/ROLIM Analysis Procedures	52
4. Essential Elements of MOSTAB Math Models	53
5. MOSTAB Executive Logical Procedure	54
6. Fundamentals of Rotor Analysis	55
7. Aeroelastic Blade Analysis	56
8. Gimbal Analysis	57
9. Advanced Shadow Model	58
10. MOSTAB Outputs	59
11. Steps in ROLIM Process	60
12. The Rotor Linear Modelling Program ROLIM	61
13. Example ROLIM Printouts	62
14. Tower Math Model	63
15. Sample Control System Model	64
16. Power Train Dynamic Math Model	65
17. Wind Turbine System Block Diagram	66
18. Long Yoke Teetering Design	67

19.	Short Yoke Teetering Concept	68
20.	Linkage Teetering Concept	69
21.	Root Out-Of-Plane Moment	70
22.	Root In-Plane Moment	71
23.	Blade Tip Deflection	72
24.	Blade Moment Reduction Expected from Teetering as a Function of Present Hub Support Stiffness	73
25.	Elastic Interface Flexure A	74
26.	Elastic Interface Flexure B	75
27.	Elastic Interface Flexure C	76
28.	Elastic Interface Flexure D	77
29.	Root Out-Of-Plane Bending Moment	78
30.	Root In-Plane Bending Moment	79
31.	Blade Tip Deflection	80

COUPLED DYNAMICS ANALYSIS
OF WIND ENERGY SYSTEMS

John A. Hoffman
Paragon Pacific, Inc.

SUMMARY

A qualitative description of all key elements of a complete wind energy system computer analysis code is presented. The analysis system addresses the coupled dynamics characteristics of wind energy systems, including the interactions of the rotor, tower, nacelle, power train, control system, and electrical network. The coupled dynamics are analyzed in both the frequency and time domains to provide the basic motions and loads data required for design, performance verification and operations analysis activities.

Elements of the coupled analysis code were used to design and analyze candidate rotor articulation concepts for the NASA/ERDA Mod O Wind Turbine System. Fundamental results and conclusions derived from these studies are presented.

INTRODUCTION

This report presents a comprehensive description of a complete wind energy system digital computer analysis code. Also presented are fundamental analysis results produced by the coupled dynamics programs, as applicable to the NASA Mod O Wind Turbine at Sandusky, Ohio. The analysis results address the baseline Mod O system and variations from this baseline design associated with various rotor articulation concepts.

The fundamental emphasis of this report is directed toward a complete definition of the wind turbine system computer analysis, focusing on the assumptions and procedures of the methods and the types of problems the system can solve. The detailed equations and logic coded in the analysis programs and the user's information required to effectively use these codes, being very voluminous, are provided in References 1 through 3, inclusive.

Evolution of the Wind Energy System Analysis Codes

The wind energy system coupled dynamics analysis program was developed using existing methods and codes synthesized originally for application to rotorcraft. The MODular STABility Derivative Program (MOSTAB) series and the Rotor LInear Modelling Code (ROLIM) represent the contributions of these original analysis systems. MOSTAB and ROLIM were developed over a period of many years, and found financial support from a number of sources. Table I presents a brief history of the developments of these baseline codes, for general reference.

An early version of MOSTAB, MOSTAB-C (M-C), was first converted for application to wind energy system analysis. This program, MOSTAB-WT, has been used extensively for wind turbine rotor performance and preliminary loads analysis. The analysis methods and procedures incorporated in MOSTAB-WT have been documented in Reference 4. References 5 and 6 present results derived in part, using MOSTAB-WT, as these apply to various phases of wind energy system analysis.

Although MOSTAB-WT provided much useful information about wind turbine performance and dynamics, it was recognized that much more advanced analysis methods would eventually be required for comprehensive treatment of these complex dynamic systems. MOSTAB-WT includes the dynamics of the first flap-ping mode of the blade - considered adequate for most performance examinations and for preliminary motions and loads analysis. The rotorcraft technology suggested the extreme importance of higher frequency blade dynamics, however, as these affect dynamic loads, overall system aeromechanical stability, and dynamic response performance. Additionally, MOSTAB-WT assumed the "fixed shaft" environment, wherein the rotor shaft centerline is presumed fixed in space, and that the rotational speed of the shaft is maintained perfectly constant. Test data taken from the MOD O Wind Turbine, and past experience in the rotorcraft technology, suggested that the fixed shaft assumption would mask critical dynamic phenomena that occur through couplings among rotor blade, support system, power train and control system degrees of freedom.

The early recognition of MOSTAB-WT limitations for comprehensive wind turbine dynamics analysis instigated the contractual work defined herein, which has provided a complete series of coupled dynamics analysis codes applicable specifically to wind energy systems. This advanced system started with the MOSTAB-HFA version (-HFA denoting High Frequency Analysis). MOSTAB-HFA is a rotorcraft analysis code that includes high frequency rotor blade degrees of freedom. Additionally, the coupled system analysis includes*the Rotor Linear Modelling Program (ROLIM) as a key element. ROLIM uses the complete nonlinear rotor models in MOSTAB-HFW (-HFW standing for the high frequency wind turbine conversion of MOSTAB-HFA) to synthesize a rigorous linear rotor model in periodic coefficients. The ROLIM model is then combined with linear models for other key system components to produce the overall coupled system model required for advanced dynamic analysis of wind energy systems. The coupling code has been given the name WIND energy Linear Analysis Software System (WINDLASS). The complete analysis system has been named MOSTAS, an acronym derived from MOSTAB and WINDLASS.

Fundamental Objectives for the Coupled Dynamics Analysis Code

The basic objectives of the coupled analysis can be grouped essentially into three categories: stability, loads and performance.

Stability refers to the tendency of the various degrees of freedom of a system to seek a steady-state and bounded excitation, once set in arbitrary motion. If a system is unstable, one or more system degrees of freedom will diverge without bound until either nonlinearities intervene to limit the motion or (usually catastrophic) failure of system elements involved in the motion occurs. The rotorcraft technology has many kinds of aeromechanical/control system instabilities that have been well publicized, including ground resonance, flap-lag instability, classical blade flutter (flap-torsion) and various instabilities associated with control system interactions. Many obvious similarities between rotorcraft and wind turbine systems can be cited. These include the large aeroelastic rotor mounted on flexible supports, with relatively tight-looped control system elements. Hence, one might strongly suspect that wind energy systems possess an affinity for aeromechanical and control system interactive instabilities. In fact, the wind turbine might tend to be even more prone to regions of instability in some cases because of the widely varying operating conditions involved. An example of this is rotor speed, which is tightly bounded to within a small variation from a nominal speed in the case of rotorcraft in flight, while the wind turbine may operate over a relatively large band of speeds.

Because of the stability considerations addressed above, stability assessment of the coupled wind energy system dynamics represents a key requirement on the comprehensive analysis code.

* At the time of this writing, the ROLIM system and its associated documentation (Reference 2) are proprietary, with distribution limited to governmental agencies only.

Loads and associated motions of the various system degrees of freedom have a major impact on system component design. Test data gleaned from experimental operation of the Mod 0 Wind Turbine has shown that blade loads, for example, can be significantly influenced by the dynamic variations of shaft position and rotor speed. This conclusion would also be indicated from past rotorcraft experience. Thus, the assessment of critical component dynamic loads is seen to depend on the coupled interactions among the various components of the wind energy system. Tower and nacelle dynamic characteristics will allow the shaft to move in space as the rotor turns and develops time-varying blade shank loads. Flexibilities in the power train provide for time-varying rotor speed, as dynamically varying shaft torques produced by the rotor excite the power train elements. It is likely that loops in the wind turbine control system, responding to the time-varying actions of the rotor, power train and supports, may also participate in the coupled dynamics in a significant manner.

From these considerations, one places an important requirement on the coupled analysis: to predict loads and motions associated with key dynamic elements of the wind energy system, including the critical interactions of its various components.

Performance is often thought simply to be the average power produced by the wind energy system in a given environment; in a dynamic context, however, the term "performance" receives a broader interpretation. When the wind turbine operates in its highly asymmetrical environment, which includes excitations from the tower shadow,* wind shear and oblique wind approach velocities, the coupled system components can respond to produce dynamically varying power output levels. Hence, the dynamic performance of the system refers to its ability to produce power of usable quality. If the power is delivered as alternating current (AC) that is to be applied to an existing utility network with an established frequency and phase angle, the wind energy system must be precisely controlled to deliver the AC power at acceptable frequency, phase angle and purity (from spurious constituents) to be usable and efficiently consumable. The coupled dynamic performance of all elements of the wind energy system and, specifically, the rotor, power train, electrical equipment and control system must, therefore, be carefully considered.

In the context addressed above, dynamic performance assessment becomes a critical requirement on the coupled analysis code.

Other types of dynamic analysis results, in addition to those addressed above, can be gleaned from the analysis program addressed by this report; some of these results, of course, may require some program refinement, while others are natural components of the existing program output. The specific types of analyses that can be performed by the code and the associated limiting assumptions are addressed in the remaining sections of this report. The current analysis system has been developed to achieve the key goals listed above, however, and these are to be considered the major types of solutions that can be found on a routine basis, using this advanced computer software.

* The tower shadow effect is the dynamic excitation of rotor blade loads and motions when the blades pass through the wake of an upwind tower.

Design and Analysis of Candidate Mod-O Rotor Articulation Concepts

A component of the subject contractual activity addressed the preliminary design and computer analysis of candidate rotor articulation arrangements for the Mod O Wind Turbine system. Two classes of devices were considered: the teetering suspension and blade-root elastic interfacing devices. Both classes of devices were examined for the fundamental purpose of reducing blade loads of the Mod O unit, thereby extending the fatigue life of the blades. The devices were to be "bolt-on" units, involving minimum modification of existing Mod O hardware.

Completed elements of the coupled dynamics software were used to analyze the candidate designs during the period when the full coupled analysis was being developed. Time was of the essence. The results gleaned from application of these analysis codes were used to derive the key conclusions associated with each candidate device.

Reference 7 represents the detailed design and analysis documentation developed for the Mod O articulation concepts. The key results and conclusions are summarized in a later section of this report, under the heading "Design and Analysis of Candidate Mod O Hub Articulation Concepts."

Organization of the Remaining Sections of this Report

The next section of this report presents a global description of the wind energy system analysis code. The data interfaces among the several elements of the code, each of which is executed separately in the complete analysis, are shown. The fundamental assumptions and procedures incorporated in the various executive sections of the overall system are addressed, and the extent and validity of the results produced by each section are identified. Alternative analysis procedures which could be implemented are also addressed, and the fundamental reasons why the approach taken for the coupled analysis was selected from the candidates are given.

A description of each element of the coupled analysis code is then presented. Basic logical procedures incorporated in each segment are addressed. Assumptions and methods incorporated in the various analyses are addressed in more detail than presented previously.

The next section presents a summary of the results and conclusions derived during the design and analysis of the Mod O rotor articulation concepts.

Finally, recommendations for further research, which address practical extension and refinement of the current wind energy system analysis software, are extended in the remaining section of the report.

OVERALL SYSTEM DESCRIPTION - WIND ENERGY SYSTEM COUPLED DYNAMICS ANALYSIS CODE

This section summarizes the operation of the total analysis system, concentrating on the data interfaces and analysis results from each subsystem. A discussion of candidate analysis procedures is also presented, identifying the basic reasons for taking the selected approach.

Overall System Arrangement

Figure 1 is a block diagram depicting the overall system arrangement currently incorporated in the coupled dynamics analysis software. Each rectangular block represents an independent executive computer code. With the input data provided, as indicated, each of these programs can be executed to completion, producing essential output information in each case. The hexagonal figures indicate data read from cards by each executive subsystem, and the curved figures summarize the information printed by each subcode. Other data interfaces, indicated by lines, are tape or disk files.

The system has been arranged as indicated by Figure 1 for economy. Since the full wind energy system analysis can be performed in a series of independent steps, the steps are executed separately to minimize the required use of computer storage. Additionally, when a series of analyses is being performed, subcodes need to be executed only when a change has occurred in its input data. Often, an entire series of analyses can be performed by serially executing only one or two of the five basic subcodes.

To see the storage use features of this arrangement, consider the storage requirements. System DATAIN is essentially an Input/Output (I/O) function which reads the basic MOSTAB input data and verify-writes the data in a formatted printout. Such an I/O function is required only when the MOSTAB data changes; an appreciable amount of storage is involved in this I/O operation, engaging relatively complex FORMAT statements that are not needed by any of the other subcodes. Hence, when the DATAIN execution is complete, its presence in storage is destroyed, making that storage available for use by other subcodes.

Similar explanations apply to the other subcodes in the system. For example, MOSTAB-HFW involves the use of considerable storage for the complex rotor blade math models, including the nonlinear inertial and aerodynamic distributed loading functions, radial and azimuthal numerical integration algorithms, etc. Once the trim condition is found by MOSTAB and the loads and motions data (the PROCES file) and the linear model (the ROLIM file) are produced, the complex MOSTAB models are no longer required, and can be unloaded.

Executive efficiency is also enhanced by the arrangement of Figure 1. For example, suppose the coupled system analysis is being used to investigate the effect of a flexible coupling stiffness in the power train. A series of analyses are to be performed at various operating conditions, as the stiffness

is varied. In this case, the DATAIN/MOSTAB/PROCES/ROLIM executions need to be made only as the wind environment and rotor speed are changed. These analysis executions result eventually in a series of ROLIM math models, probably stored permanently on tape or disk. These same models can be used over and over again as the power train design is changed. The linear analysis would be re-executed for the series of operating conditions (on the ROLIM file) at each stiffness value. Overall system stability, loads and dynamic performance would be determined for each stiffness value, by successive re-execution of a comparatively small portion of the total analysis software system.

The ability to segment the analysis in a manner optimized for system component synthesis (as exemplified by the flexible coupling project described above) is a key reason for selecting this particular analysis approach taken here. The trades between this approach and popular candidate methods are discussed in more detail in a subsequent section.

Subcode Data Interfaces

The data interfaces summarized by Figure 1 represent the input data required for and the outputs produced by each executive subcode. The data interfaces are interconnected by various media, including the card reader and punch; tape, disk and drum files; and the line printer. Table II presents a summary description of these data interfaces serving to define, in qualitative terms, the input data requirements of each subcode and the useful data produced by each module.

Sequence of Events - Coupled System Analysis

The software system typically operates according to the series of events described below, in performing a complete coupled analysis. This series could be implemented as one computer job with the described series of individual executions or, perhaps more likely, the user would inspect intermediate job steps prior to the instigation of successive computational tasks. As mentioned above, all subcodes will generally not require execution for a series of analyses.

DATAIN execution will use the basic MOSTAB input data defined in detail in Reference 3 and qualitatively by Table II. This step is low risk and would fail only if input data errors are encountered or if the input data prepared by the user exceeds prescribed storage limitations. The DATAIN results will be printed, and a tape or disk file will be created for access by the next executive subcode: MOSTAB-HFW.

MOSTAB-HFW, upon reading the DATAIN file, attempts to find a "trim" solution. Trim occurs when compatible sets of rotor loads and wake variables have been determined and when a blade-motion history (as a function of rotor azimuthal position) has been determined which is periodic. If a gimballed rotor analysis is being performed (e.g., teetering or floating hub rotor articulation arrangements), the "gimbal error" function described in

Reference 2 must also be driven to zero within acceptable limits. This analysis step represents the most hazard to the success of an overall system analysis, due to potential failure of the trim-search process. The trim search can fail if input data estimates are so far from the true case as to drive the rotor airfoils into areas of extreme nonlinearity (stall). If this happens, a successful trim search can almost always be achieved by rerunning the case with improved estimates.

MOSTAB-HFW prints the key results of the trim-search process and also generates two disk or tape data files, as indicated by Figure 1. These files are processed by the successive executions of subcodes PROCES and ROLIM.

PROCES is a relatively simple subcode, which reads the PROCES data file produced by MOSTAB-HFW and prints the data as a function of blade azimuth and radius. Only four cards are read by PROCES: three of which are arbitrary title cards and one of which is a data file unit number and executive option index card. This submodule presents essentially zero risk to successful completion unless there are errors in the input data - no indeterminable outcome events (e.g., iterations) are involved.

PROCES performs a harmonic analysis of the blade loads for convenience. This relatively small and simple subcode will probably be modified from time to time by the user to perform various functions on the loads and motion data. For example, a relatively simple algorithm can be devised to scan the data and select maximum and minimum loads (for a full azimuthal sweep) at selected radial stations of interest. In this way, the relatively large PROCES data file can be reduced to a small set of relevant numbers, say, for input to cumulative fatigue damage analyses.

ROLIM performs a series of complex data processes using standard matrix procedures. The single blade linear math model produced by MOSTAB-HFW (ROLIMX), for example, is expanded to represent all blades in the rotor. The blades are aerodynamically coupled by the linear wake models, also produced by ROLIMX.

Despite the relative complexity of the ROLIM processes, they do not involve indeterminable-outcome events (iterations, numerical integrations, etc.), so that the ROLIM processes will occur with minimum failure risk. The user-prepared card inputs to ROLIM are very abbreviated (five cards, three of which are title cards, and the rest of which involve various executive option indices).

The system user will probably execute a series of MOSTAB-HFW/PROCES/ROLIM cases and create a ROLIM data file series, representing the operation of a given wind turbine system for varying wind and rotor speeds. These data series can then be used repetitively by the coupled system linear analysis subcode.

The Coupled Dynamics Linear Analysis Subcode reads the ROLIM data tape, and a relatively substantial amount of system physical data from cards, and assembles the linear system equations. This portion of the coupled system analysis involves matrix processing, which derives linear math models for all system components (except the rotor) from cards, and combines these with the ROLIM rotor model to yield the coupled system equations.

Two coupled system equation sets emerge and these are combined to eliminate a group of "removable" variables, to yield a single linear equation of the form:

$$\ddot{Mw} + \dot{Bw} + Kw = W_v v$$

where w is a column of system degrees of freedom, including contributions from the rotor, tower, power train and control system; v is a column of externally defined variables and includes such items as control system rotor speed input commands. The upper case notation in the equation represents constant matrix operators.

The eigenvalues of the lefthand side of the dynamic equation reflect the system stability characteristics, so these are computed in the analysis. The forced response of the equation is calculated by including the shaft and torque loads generated by MOSTAB-HFW, in v . Recalling that the MOSTAB-HFW loads assume a fixed shaft and constant rotor speed, one sees that the w response to these loads represents the result of shaft motion. Superimposing the fixed shaft loads with the perturbation loads yields the full coupled system loads. These computations are made in the linear analysis subcode in the time domain and output to the line printer.

Fundamental Assumptions Incorporated in the Analysis

Each subcode depicted by Figure 1, of course, contains its own basic assumptions. These are partially identified in the next major section and, in detail, in References 1 through 3. There are a series of global assumptions, however, that one might identify as being applicable to the analysis system as a whole. These are listed below.

Superposition - The MOSTAB-HFW execution involves a full nonlinear set of equations that are solved for a given operating condition, presuming a fixed shaft, quiescent control inputs and constant rotor speed. Then, the coupled system analysis is performed using linear models, and the linear and quiescent (MOSTAB-HFW) motions and loads solutions are then superimposed to yield the final loads and motions results. If the shaft, control system or power train degrees of freedom become excited to extreme amplitudes for a particular operating condition, some nonlinear phenomena may become involved. In such a case, which can reasonably be considered very unusual, the superimposed results may be somewhat in error. As described in the final section of this report, under "Recommendations for Further Research," key nonlinearities can be added to the coupled system analysis and executed in the time domain, thereby removing associated errors resulting from the superposition process.*

* It is also possible to "loop back" to MOSTAB-HFW with the calculated shaft-motion results, to recompute loads and motions using the full nonlinear system models. The looping could be recursive for convergence to an exact solution, if necessary in rare instances.

Constant Coefficients - Reference 2 describes the process in ROLIM wherein the rotor linear models are transformed to multi-blade coordinates, thereby removing the once-per-rev components in the operators. This process leaves the operators with substantial constant coefficient constituents and some "n-per-rev" constituents, where n is the number of blades in the rotor. This process justifies the use of the constant coefficient portion of the rotor model in many instances, neglecting the two- and higher-per-rev elements. In some cases, however (particularly in the case of rotors with two blades, which lack diametrical inertial and aerodynamic symmetry), the time-varying elements should be considered. Floquet analysis can be used to treat the time-varying coefficients in the stability analysis (see Reference 8), and the inclusion of these elements in the time domain portion of the coupled analysis is straightforward.

Alternative Analysis Methods

Many important reasons exist for selecting the analysis procedure described herein over candidate methods. Some of these reasons and some significant trades involved in selecting methods are discussed in this section.

Perhaps, the most common alternative selected in the rotorcraft field* for solving the complete coupled system dynamics problem is the digital simulation procedure. In the simulation, math models for each system component are solved in the time domain. The numerical integration of degrees of freedom in all components of the system occurs in a serial fashion with results latched together at the end of each numerical integration time interval. Hence, a time step advancement begins at an instant where all component state variables and interfacing loads are specified. With the applied loads known, the state variables in each system component math model are advanced over one numerical integration time interval, using one of many algorithms for the advancement. At the end of the interval, the interfacing loads are calculated based on the newly advanced values of each component state vector and the process is then repeated, serially, to yield time-history records of the system response.

The simulation has the advantage that nonlinearities can be included in each system component math module, and the calculated results reflect these nonlinearities. Additionally, the full influence of the time-varying rotor phenomena is theoretically included.

In spite of these significant advantages, the digital simulation has many serious problems, which tend to limit the practical utility of such methods. A few of these problems are listed on the following page.

*In the rotorcraft problem, the rotor, nonrotating airframe, propulsion system and flight control system relate analogously to the wind turbine rotor, tower, power train and control system elements.

Cost - The models in the simulation must all be executed simultaneously, to yield the final time-history results for a given operating condition. Some of these models (e.g., the rotor model) are very expensive to solve because of their complexity, but still must be constantly re-executed in the simulation, even when the environmental conditions and physical parameters associated with the model do not change. This limitation raises the costs of operating the simulation so drastically, in many cases, that the practical utility of the simulation is very limited. A given analysis activity can usually afford to produce only a few results within the cost and scheduler constraints involved, if a digital simulation is used.

Stability Assessment - Figure 2 presents a typical time history trace that might be produced by a digital simulation. The enveloped high frequency response characteristic is typical when aeroelastic rotor models are involved. To assess the stability of the system, a relatively extensive time-history trace must be run, to determine the final response of the low frequency "envelope" modes. Yet this costly process yields only a single result - whether or not the system is stable for the given parameters and operating conditions. The relative stability (or the severity of the instability) is not indicated. Stability boundaries can be found using many (long) time-history traces to establish only a single boundary point!

Frequency domain techniques, also depicted by Figure 2, show the exact positions of the system characteristic roots, revealing the stability margins for each mode. Classical control system techniques such as root-locus and Bode methods can be used to show variations in relative stability as key system parameters are synthesized. Hence, one sees that the frequency-domain techniques offer significant advantages over the time-domain approach, when system stability is being evaluated. These comparative advantages are summarized by Table III.

Numerical Problems - Digital simulations suffer from a whole series of numerical problems which, at worst, can yield the simulation inoperable or, in many cases at least, can introduce significant errors in the calculated results. A detailed discussion of these problems extends beyond the scope of this report. They are treated in more detail in Reference 9. In summary, these problems can be grouped as follows:

- 1) Stability Aberration: Numerical integration processes have the well known tendency to modify the basic stability of a dynamic mode because of the computational lags associated with numerical integration. Lightly damped modes, which are common in structural systems such as wind energy machines, can be driven unstable in a digital simulation. Often, digital simulation users have to add "artificial" damping to such troublesome modes, a process that sheds considerable doubt on the final simulation results;
- 2) Coupling Instabilities: Many types of numerical instabilities, or stability aberrations such as those discussed above, occur when fundamentally sound system component models are coupled together.

Because of the computational lags associated with the interfacing forcing variables, a coupled assemblage of stable modules can go unstable when coupled together. Simulation users sometimes interject nonphysical digital filters between troublesome modules, a process which also sheds considerable doubt on the final simulation results.

Because of the many problems associated with digital simulation, the alternative procedure addressed by this report has been selected for comprehensive analysis of wind energy system dynamics. The basic elements of the analysis method shown by Figure 1 represent those required for digital simulation, however. Hence, relatively straightforward modifications could link these constituents together in the time domain, to form a simulation. The resulting software system would, of course, be subject to the drawbacks and problems listed above.

COMPONENT MODEL DESCRIPTIONS

The previous section presented a global description of the wind energy system coupled dynamics analysis, showing data interfaces and describing the operation of each system subcode in abbreviated terms. This section presents a more detailed discussion of the methods, procedures and assumptions incorporated in each analytic subcode.

Datain

Being essentially an input/output utility code, DATAIN requires no additional discussion in this section.

Mostab-HFW

Figure 3 presents the basic procedures incorporated in MOSTAB-HFW, including the interfaces with PROCES and ROLIM addressed in the preceding section. As described before, MOSTAB-HFW reads the essential physical and operational data specifications and then determines a "trim" condition using a full set of system component math models. After trim is found, these non-linear models are used by a group of subroutines managed by S/R ROLIMX, to produce the generic linear modelling data required by ROLIM. Rotor data at trim is output for later handling by subcode PROCES, as shown by Figure 3.

Figure 4 presents a more detailed logical definition of the MOSTAB math models. The "FORCE" models which include the complex aeroelastic rotor equations shown in the dashed box, produce all system loads, and the blade dynamic motions, given the velocity, acceleration and control environment. The interference velocity components, on the other hand, are produced by "WASH," given all the system loads. Hence, the MOSTAB executive system iterates the FORCE and WASH models to converge to compatible load and velocity

sets: essentially representing a simultaneous algebraic solution of the full nonlinear force and velocity math models.

Figure 5 presents more detail on the executive logic procedures incorporated in MOSTAB-HFW. The trim-search loop makes successive estimates of the interference velocity variables which are improved until convergence occurs. After trim is found, key results are printed, the PROCES file is created and, finally, ROLIMX creates the linear models needed eventually by the ROLIM processor. ROLIMX generates a linear model for only one rotor blade. This full model, which relates blade motion forcing functions and shaft loads created by the blade to all blade, shaft and control degrees of freedom, is created at each azimuthal station used in the blade motion numerical integration process. ROLIMX also synthesizes linear models for the wake, using the "WASH" math models.

The most complex part of the MOSTAB analysis is that used to treat aero-elastic rotors. Figure 6 presents the coordinates and some key assumptions incorporated in MOSTAB rotor analyses. The motion of the blade reference line is calculated as a function of blade azimuthal position using a modal analysis of blade dynamics (see Reference 10 for a discussion of this method of structural dynamics analysis). These motions and all internal and shaft loads supported by the blade are computed by finding the distributed aerodynamic and inertial loads applied to the Blade Reference Line (BRL) at each azimuthal station used in the numerical integration process. These loads, of course, are functions of the BRL position, velocity and acceleration as a function of radius, and of the shaft and control system variables (velocities, accelerations and positions). The distributed loads are integrated radially, at each azimuthal station, to produce the required BRL, shaft and internal blade force and moment components.

Figure 7 presents a list of key assumptions and procedures incorporated in the MOSTAB-HFW analysis.

Figure 8 presents a key addition to MOSTAB-HFW system made as part of the subject contractual activities. Previous versions of MOSTAB only analyzed rotors where the blades were fully isolated by the shaft. In this case, a full rotor can be analyzed by solving for the loads and motions of one blade, since the shaft motions (and rotor speed) are prescribed and the trim-search process provides for a periodic solution wherein all blades do the same thing at different phase angles. The gimballed rotor cannot be solved this way since the blades are dynamically coupled by the gimbal housing degrees of freedom with respect to the shaft.

The MOSTAB-HFW gimbal analysis uses a single blade model to iteratively determine the motions of the gimbal housing with respect to the shaft. Figure 8 depicts this iterative process, wherein a "gimbal error" function (e.g., the moment about a teetering bearing produced by all blades in the rotor) is driven to zero through successive iteration passes. The gimbal iteration process occurs in parallel with the overall MOSTAB-HFW trim-search iteration; i.e., one pass through the gimbal iteration occurs per every trim-search pass.

Figure 9 represents another major modification made to earlier MOSTAB versions, specifically to treat special wind turbine phenomena. The shadow wakes behind wind turbine towers tend to be very impulsive as they influence blade motions. Hence, very small azimuthal integration steps are required to properly determine the influence of the shadow wake on blade motions. Unfortunately, such small steps are very expensive, particularly if they are used around the entire azimuth.

The advanced shadow model now incorporated in MOSTAB-HFW, and represented by Figure 9, uses sub-sectored numerical integration intervals in the shadow region. Additionally, the shadow wake is specified as a complete map, with retardation velocities varying with radius and with azimuth in essentially any arbitrary manner, to embrace the complex wake profiles developed behind wind turbine towers of varying shapes.

Figure 10 summarizes the key output data generated by MOSTAB-HFW. Much of this data is usable in its own right, while other constituents of the data are used as inputs to other submodules in the overall wind energy system dynamic analysis code.

Rolim

The ROLIM processor generates a linear math model in periodic coefficients, representing the rotor system, including rotor blade aeroelastic degrees of freedom.

Figure 11 lists the steps taken by the ROLIM processor in generating the model, and Figure 12 presents the math model as a matrix equation. Because the rotor turns, the elements in the linear operators are periodic functions of time. Figure 13 presents a small portion of the ROLIM printout, showing a few elements of the matrix operator Y_{Ω} as they vary about the azimuth.*

The ROLIM model is placed on disk or tape for future processing by the linear analysis subcode, as shown by Figure 1.

The Coupled System Linear Analysis (WINDLASS)

MOSTAB-HFW, ROLIM, and their associated subsystems deal with the computation of fixed-shaft rotor loads and motions and a linear math model of the rotor valid for perturbations of the system variables with respect to the MOSTAB-HFW fixed-shaft solution. The coupled linear analysis subcode generates math models for the other wind energy system components, combines these and finds linear solutions of the coupled equations. The paragraphs that follow address the generation of the component math models and then their combination solution.

* PSI = azimuth angle of rotor blade number 1; $\psi = 0$ is blade down in the wind turbine application.

System Component Math Models - The linear analysis subcode reads physical properties of the tower, control system, power train and pod from cards, generates their corresponding linear equations, and stores these for further processing. Some of the basic procedures and assumptions incorporated in these models are summarized below.

1) Tower Model

The tower model is depicted by Figure 14 and is a superposition of two independent linear representations of this structure. A modal model of the tower, which presumes a fixed tower base, is mathematically superimposed upon a rigid tower model on a flexible base. The modal model is defined as a series of tower modeshapes and frequencies, along with a definition of the mass properties. Flexibility properties are not required. The modal entities required are compatible with those routinely generated using finite element structural analysis codes such as NASTRAN.

The modal properties of the tower would most likely be generated (using NASTRAN, for example) assuming a fixed or perfectly rigid base. The tower modal properties depend only on the wind turbine design, while the base properties could be influenced by the installation site soil properties.

To allow a standard modal model for a tower of a given design to be used for analyses including soil properties, the flexible-base model has been added. The influence of such a flexible base on overall system dynamics can be included by combining the base model coupled to a rigid tower, with the modal model valid for a fixed base. Rigid-body tower motions on the flexible base produce distributed loads on the modal model, through accelerations times the tower mass properties. The final coupled model is rigorous, within the frame of the basic assumptions used in the base and modal formulations and, of course, the assumption of linearity.

The tower modal analysis should include a mass at the top approximating the mass properties of the nacelle-rotor unit. The resulting modeshapes and frequencies will then reflect a more accurate representation of tower dynamics in its actual operating environment. The effect of this mass will, of course, have to be subtracted from the actual loads applied to the tower by the nacelle (pod) at the pod/tower interface.

2) Control System Model

The control system model represents the power machinery, power machinery controls, utility network dynamics, rotor speed controller, and any other servo systems considered significant to overall wind energy machine performance. Figure 15 shows a block diagram which might be used to represent such a system. The control system is first defined in transfer-function block diagram form; the transfer functions are then codified using a straightforward procedure, and read by the linear subcode. The codified control system model is

converted to a time domain state space matrix equation in the linear analysis module, for convenient interfacing with the other wind energy system models.

3) Power Train Model

The power train model is defined as an assemblage of linked modules, such as depicted by Figure 16. Each module contains a gear ratio, an inertia, a stiffness and two damping coefficients for series and parallel damping effects, as shown. The modules can be linked together in any arbitrary way, using a linking code read by the linear analysis software. This modularized definition of the power train is very general and can embrace most known methods for transferring and branching mechanical power.

Upon reading the coding indices and physical data for the power train, the linear analysis subcode generates a linear matrix equation in the time domain, representing the power train dynamic characteristics.

4) Pod Model

The pod, or nacelle, can be looked upon as an interfacing device that connects the rotor, power train, tower and control system units together. The pod model incorporated in the linear analysis package is a superposition, very similar to that used for the tower. The pod is assumed to be a massless elastic body - a pure spring with multi-degrees of freedom, superimposed with an infinitely rigid mass. Hence, the pod has no relative mass/elastic modes, but does contribute its mass properties to the overall system dynamics and does interface the other system components elastically.

Because the pod is so small and stiff compared to other components of the wind energy system, its mass/elastic natural frequencies can be expected to be extremely high compared to the other significant dynamic modes of the system. In other words, the pod will interact with the other components as an elastic system with rigid-body mass properties. The presence of such high frequency modes in an analysis can produce serious numerical problems, in either the frequency or the time domains, when an attempt is made to solve the coupled dynamics equation. Their presence will have no significant influence on a correct solution, however, for the fundamental coupled dynamics characteristics of interest. Hence, to prevent such classical numerical problems, the pod relative modes have been omitted from the coupled model.

Combining the Linear Models - Previous sections of this report have discussed the individual linear models synthesized for each major component of the complete wind energy system. Each component model, and the software developed to synthesize it, has been developed to be as general as possible, in order to embrace as many future variations in wind machine design as possible.

Once the component models are available, the linear analysis software combines them into an overall system model. Figure 17 is a block diagram showing the individual models, their interfacing expressions, and their interfacing data paths. The symbols of Figure 17 are defined in Tables IV, V, and VI. One sees that the complete system is made up of many variables and matrix operators, linked together in a prescribed manner.

The assembly code has been developed to be extremely general so that changes to the specific arrangement of Figure 17 can be easily incorporated with minimal or no source code modification. In other words, the assembly code is programmable by the user, as if it were a higher level compiler, to assemble the constituent system math models in virtually any arbitrary manner.

The general assembly code is programmed by user specification indices read by the system. These indices perform the following functions:

- a) Categorize all problem variables into three groups: independent variables, removable variables (i.e., variables that can be fully defined as linear functions of the other two variable groups) and external or forcing-function variables.
- b) Number all of the matrix equations in all of the constituent models of the system, including the interfacing equations.
- c) Number all of the matrix operators in the equations.
- d) Specify the dimensions of the operators; i.e., the number of rows in each matrix equation and the number of rows in each variable column vector.
- e) Specify scale factors to be applied to the individual variable column vectors, to protect subsequent analysis steps from numerical difficulties.
- f) Specify the locations (disk or tape unit numbers and relative storage addresses for "in-core" residency) of all the operators in the component models.

With these user-specified indices, the assembly code generates two equations of the form:

$$C_{\dot{w}} \ddot{w} + C_{\dot{w}} \dot{w} + C_w w = C_e e + C_v v \quad (1)$$

$$E_e e = E_{\ddot{w}} \ddot{w} + E_{\dot{w}} \dot{w} + E_w w + E_v v \quad (2)$$

where

- w = column vector of all independent variables in the problem, included as stacked subvectors;
- e = column of "removable variable" subcolumns;
- v = column of externally supplied excitation functions, including such items as control commands and the shaft loads produced by MOSTAB-HFW assuming a rigid shaft, constant rotor speed and quiescent control input.

The upper case notation represent the constant matrix operators, assembled by placing the smaller operators in the blocks of Figure 17 into the overall system operators of Equations (1) and (2). The assembly codification indices discussed above enable the software to place the constituent matrix operators in the proper places within the overall system operators.

With Expressions (1) and (2) available, the column e is removable using straightforward matrix procedures. E must, of course, be invertible. After the removal (elimination), the final coupled dynamics equation appears as:

$$\ddot{M}w + \dot{B}w + Kw = W_v v \quad (3)$$

where the new operators are given by

$$M \triangleq C_w - C_e E_e^{-1} E_w \quad (4)$$

$$B \triangleq C_w - C_e E_e^{-1} E_w \quad (5)$$

$$K \triangleq C_w - C_e E_e^{-1} E_w \quad (6)$$

$$W_v \triangleq C_v + C_e E_e^{-1} E_v \quad (7)$$

Note that the solution of Equation (3) can be substituted into Expression (2) to yield the removable column, e.

Solving the Linear Model - Equation (3) represents the coupled system math model, and can be solved using a number of different linear analysis techniques. As a general rule, the operators in Equation (3) will be periodic functions of time,* since they contain contributions from the ROLIM operators which are time varying. In this case, the full assembly process described above must be re-executed at each rotor azimuthal station - each station represented by a different ROLIM model.

The solutions to systems of linear equations are synthesized in two steps: the homogeneous solution and the particular solution. These independent steps are discussed below.

1) The Homogeneous Solution

The homogeneous solution is the solution to Equation (3) with right-hand side set to zero. The resulting equation is first reduced to first order, to have the form:

$$P\dot{y} - Qy = 0 \quad (8)$$

where

$$y = \begin{pmatrix} \dot{w} \\ w \end{pmatrix} \quad (9)$$

$$P \triangleq \left[\begin{array}{c|c} 1 & 0 \\ \hline 0 & M \end{array} \right] \quad (10)$$

$$Q \triangleq \left[\begin{array}{c|c} 0 & 1 \\ \hline -K & -B \end{array} \right] \quad (11)$$

One would wish to invert P and premultiply through by P-inverse to reduce Expression (8) to the usual characteristic equation form. Because of the nature of the wind turbine system math models, however, P is generally singular. Q will also be singular, in general, and the specific ranks of these arrays will depend on the detailed models used for the wind machine components.

* At the time of this writing, the analysis system has been configured to incorporate the constant portions of the ROLIM model only, in the operators of Equation (3).

Hence, it is necessary to process Equation (8) using special procedures derived and documented in Reference 1. Singularity in P means that y is not a set of "generalized" coordinates. In other words, there are algebraic constraints among the elements of y, such that y does not contain a full column of legitimate, independent coordinates. Singularity in Q means that the system contains at least one zero eigenvalue. If Q is degenerate d times, then there are d zero (repeated) characteristic roots in the system.

The matrix procedures derived in Reference 1 essentially find a coordinate transformation matrix, T, such that the vector y can be expressed as a function of generalized-coordinate column x:

$$y = Tx \quad (12)$$

and the dynamic equation is written

$$\dot{x} - Mx = 0 \quad (13)$$

If the constant-coefficient portion of M is used, denoted herein as M_0 , then Equation (13) can be processed by straightforward eigenanalysis. If the periodic constituents in M are to be included, then the methods of Floquet must be used (see Reference 8 for a discussion of the Floquet procedure).

As mentioned previously, the constant portion of M can be used to analyze systems incorporating aeroelastic rotors, in many cases with good accuracy. In this case, one hypothesizes a solution to Expression (13) of the form:

$$x = \bar{x} e^{\lambda t} \quad (14)$$

where x is a constant vector and λ is a scalar.

Substituting this into the constant coefficient portion of Expression (13) yields,

$$(\lambda I - M_0) \bar{x} = 0 \quad (15)$$

where the symbol I has been used to denote the identity matrix.

The vector \bar{x} can have a nontrivial value, of course, only if

$$\text{Det} (\lambda I - M_0) = 0 \quad (16)$$

which is easily derived by applying Cramer's rule to Equation (13). Equation (16) is called the characteristic equation, and values of λ that satisfy this scalar expression are called the characteristic roots, or eigenvalues, of the system.

The eigenvalues, λ_j , will generally be complex numbers. If the system is stable, all the λ values will have negative real parts. If one or more λ values have positive real parts, substitution into Equation (14) clearly shows that the system is unstable.

For each eigenvalue, λ_j , there will generally be a corresponding eigenvector \bar{x}_j that is found using the eigenvalue and a pivoting numerical procedure on Expression (15).

If a Floquet procedure is used, characteristic roots, λ_j , are found that represent the basic eigenvalues of the system, with periodicity included in the analysis.

The eigenvalues are very important to the system dynamics. They show the stability (or lack thereof) of each coupled mode in the system and the relative degree of stability for each mode.

The eigenvectors show the participation of the various system components in each mode. For example, the \bar{y}_j eigenvector, defined as

$$\bar{y}_j = T \bar{x}_j \quad (17)$$

shows the coordinates in y involved in the j 'th mode of motion. If λ_j is an unstable eigenvalue, then \bar{y}_j would reveal which coordinates of the system are involved in the instability, helping to lead the system designer to an understanding and, hopefully, a correction of the instability.

2) The Particular Solution

The particular solution of Expression (3) involves solving for a specific time variable, $w(t)$, for a given forcing function $v(t)$. Then the general solution is a superposition of the homogeneous and particular solutions.

One special case of interest in the wind energy system analysis involves the particular solution of Equation (3) in response to a periodic forcing function, v . This case is particularly important in solving for the "moving shaft" system loads. In this case, v contains the periodic shaft and torque loads generated by MOSTAB-HFW, assuming the fixed shaft constraint. These loads will appear in v so that v can be written:

$$v(t) = \sum_{i=1}^N v_i e^{ji\Omega t} \quad (18)$$

where j is defined, in this case, as the complex operator.

Since Expression (3) is linear, it can be solved for each harmonic component of v considered separately, and the independently derived solutions can then be superimposed.

To see this, consider again the constant coefficient form of Expression (3). Assume a solution to the i 'th harmonic excitation from v of the form:

$$w_i = W_i e^{ji\Omega t} \quad (19)$$

Substituting Expressions (18) and (19) into the constant-coefficient portion of Equation (3) yields:

$$(-i^2\Omega^2 M_o + i\Omega jB_o + K_o) W_i e^{ji\Omega t} = W_v v_i e^{ji\Omega t} \quad (20)$$

or

$$D_i(\Omega) W_i = W_v v_i \quad (21)$$

where

$$D_i(\Omega) \triangleq (K_o - i^2\Omega^2 M_o) + j(i\Omega B_o) \quad (22)$$

The complex array D is generally nonsingular, whence

$$W_i = D_i^{-1}(\Omega) W_v v_i \quad (23)$$

Then the harmonic response to v is given by

$$t) = \sum_{i=1}^N W_i e^{ji\Omega t} \quad (24)$$

Equation (24) reveals the coupled system response to the fixed-shaft loads produced by MOSTAB-HFW. Superposition of the function $w(t)$ with the corresponding variables calculated by MOSTAB-HFW, yields the complete coupled system response with a free shaft and variable rotor speed.

The procedure described above, leading to harmonic response Expression (24), is the process currently incorporated in the coupled system analysis to produce free-shaft/speed time-history responses.

Many alterations and extensions to this method could easily be included in WINDLASS, as added developments. Two such extensions are discussed below.

3) The General Solution (Summary)

Many alternative time-domain solutions can be implemented, using the basic dynamic Equation (3). One must use caution in implementing linear analysis procedures, however, and reflect on the facts that M and K are generally singular and that all the operators are periodic functions of time. Two practical extensions of the methods currently implemented in the coupled analysis are presented below.

Either method would first convert Expression (3) to its first order form:

$$P\dot{y} - Qy = Rv \quad (25)$$

where Definitions (9) through (11) are used with

$$R \triangleq \begin{bmatrix} 0 \\ W_v \end{bmatrix} \quad (26)$$

The first procedure would simply solve Expression (25) as a constant-coefficient expression over time intervals equivalent to one rotor azimuthal station. Each successive azimuthal advance in the value of y would use entirely different linear operators, properly reflecting the periodicity in these operators.

To develop this method, one may proceed with a constant-coefficient analysis of Expression (25) since this will only be used for one azimuthal sector advance. An immediate problem is encountered, however, due to the fact that P is singular, so that one cannot solve directly for \dot{y} .

To solve this problem, the methods of Reference 1. are used to find the eigenvalues of the homogeneous portion of Expression (25). The eigenvectors are also found and stacked, column by column, in an array Y, called the modal matrix. As discussed in Reference 1, another modal matrix, Z, can be derived, such that Z is the matrix of eigenvectors for the transposed system

$$P^T \dot{z} - Q^T z = 0 \quad (27)$$

The eigenvalues of Equation (27) will be identical to those found for the homogeneous portion of Expression (25), since transposition of a determinant (Equation (16)) does not change its value.

Now specify the coordinate transformation

$$y = Y q \quad (28)$$

and transform Expression (25) accordingly. Then, premultiplying by the transposed system eigenvectors, yields

$$(Z^T PY) \dot{q} - (Z^T QY) q = (Z^T R) v \quad (29)$$

Reference 1 proves that the two operators on the lefthand side of Equation (29) are diagonal matrices, and they are nonsingular. Also, Equation (29) can be written

$$\dot{q} - \Lambda q = P_v v \quad (30)$$

where

$$P_v \triangleq (Z^T PY)^{-1} Z^T R \quad (31)$$

and

$$\Lambda = (Z^T PY)^{-1} Z^T QY \quad (32)$$

The diagonal matrix, Λ , as shown by Reference 1, has the system eigenvalues as its diagonal elements.

The array, P_v , might be called the matrix of participation factors since it determines how the forcing function elements in v participate in the excitation of each normal mode in the system. Coordinates q , which are generally complex, are called normal coordinates.

Equation (30) is solved in a straightforward manner for any arbitrary forcing function, $v(t)$, given some initial condition, $q(\tau)$, valid at time $t = \tau$. Once $q(t)$ is known, the original coordinates, y , are recovered from transformation Equation (28).

The second procedure for solving Expression (3) in the time domain, including the time-varying operators, is derived using the results of the first method. However, it does not require eigenanalysis at each rotor azimuthal station. Rather, the operators of Expression (25) are separated into constant-coefficient and time-varying component constituents. The time-varying parts are transposed to the righthand side of the equation and treated as forcing functions. The result is

$$P_0 \dot{y} - Q_0 y = P_v v - \bar{P} \dot{y} + \bar{Q} y \quad (33)$$

where the barred arrays have zero mean values. Now the entire process described for method number 1 is executed using the arrays P_0 and Q_0 .

Transformation Expression (28) is still valid and the diagonal Expression (30) emerges in the form:

$$\dot{q} - \Lambda q = P_v v + P_q \dot{q} + P_q q \quad (34)$$

where

$$P_q \triangleq - (Z^T P_0 Y)^{-1} Z^T \bar{P} Y \quad (35)$$

and

$$P_q \triangleq + (Z^T P_0 Y)^{-1} Z^T \bar{Q} Y \quad (36)$$

Equation (34) can be solved in a straightforward numerical fashion, with periodic arrays P_v , P_q and P_q known and using the constant diagonal array Λ (the eigenvalues associated with P_0 and Q_0).

In conclusion, the method of Equation (24) has been incorporated in the current coupled analysis system for time-domain examination. The alternative procedures, described above, can be implemented in a relatively straightforward manner, however, using the coupled system Equations (1) and (2) and standard linear analysis subroutines incorporated in the current system.

DESIGN AND ANALYSIS OF CANDIDATE MOD 0 HUB ARTICULATION CONCEPTS

A portion of the subject contractual activity dealt with the design and analysis of two hub articulation concepts for the Mod 0 Wind Turbine: teetering and elastic interface devices. Both concepts were investigated for their potential to reduce blade loads in the baseline Mod 0 design, and both were synthesized to involve a minimum of modification to existing Mod 0 hardware.

This section presents some of the more promising design concepts identified during the study, along with key analytical results and conclusions associated with them.

The Teetering System

Description of Concepts Considered - Figures 18 through 20 present the conceptual designs considered for the teetering systems. The system of Figure 18 places the teetering hinge forward of the point of shaft intersection with the blade centerlines, at approximately the overall rotor center of gravity point. Teetering helicopter rotors place the teetering hinge at approximately the c.g. point of the blades alone, which in the case of the Mod 0 would be about 0.91 meters (three feet) from the blade centerline intersection point. Placing the hinge outward in this fashion is called "undersling" in the helicopter vernacular; rotors are underslung to reduce the magnitude of Coriolis inplane excitation loads due to rotor teetering. The undersling shown in Figure 18 tends to reduce the Coriolis loads and, additionally, balances the complete rotor assembly for easy handling and quiet operation at near-zero speeds.

Figure 19 is the short yoke design, which makes no attempt to balance the rotor or to reduce Coriolis loads. It is much simpler and lighter than the long yoke, however.

Figure 20 presents a linkage design, which does not require a long yoke to project the virtual teetering axis well forward of the blade centerline intersection point. The device has the characteristic, however, that the virtual teetering axis does not stay stationary with respect to the shaft, but translates in an essentially vertical arc as the rotor teeters.

Table VII lists the weights and other design data associated with the teetering concepts.

Analysis Results for the Teetering System - Figures 21 through 23 present the key MOSTAB-HFW analysis results derived for the teetering concepts. Remembering that these results incorporate the fixed shaft assumption, the following observations are made:

- a) The flapwise bending loads in the teetering systems are roughly half those in the baseline (hingeless) Mod 0 design, regardless of hinge point location.*
- b) The gravity loads in the inplane direction are so large that the Coriolis loads are relatively small by comparison. Hence, "undersling" to reduce Coriolis loads, as done in helicopters, is probably of little positive consequence in the Mod 0 system.
- c) The flapwise loads remaining in the teetering rotor blade shanks are of even-per-rev harmonic content, the odd-per-rev constituents (present in the baseline Mod 0 system) being removed by teetering (as would be expected).
- d) The teetering response (Figure 23) to the shadow excitation has its maximum upwind displacement at roughly $\psi = 90$ degrees, as would be expected, and the teetering arrangement maintains the basic Mod 0 preconce. Hence, the teetering concept does not tend to allow the blades to approach significantly closer to the tower than in the baseline Mod 0 design. A gust with a vertical axis, such as might occur during thunderstorm activity, might teeter the rotor toward the tower, however.

Although the fixed-shaft analysis indicated that the teetering design could reduce flapwise bending loads by half, further examination of available Mod 0 test data indicated that the Mod 0 system is already teetering to a significant degree due to flexible shaft supports. Such flexibility probably arises from a combination of bearing, tower, pod and yaw drive flexibilities. Figure 24 shows the predicted reduction in baseline Mod 0 flapwise loads for the teetering system, including the partial reduction already made by flexible supports. This curve indicates that a teetering hub will probably reduce existing Mod 0 loads by only about 30 percent, based on estimates of the average shaft support flexibility.

Since the coupled system dynamic analysis was not available for the teetering study, the results of Figure 24 were not tested with this new and more general computer code. The results are compatible with Mod 0 test data, however, lending them considerable credibility.

The Elastic Interface Devices

Explanation of Candidate Devices - Figures 25 through 28 present four elastic interface devices which could be simply "bolted on" to the existing

* An intuitive explanation of this important result is that, when one blade passes through and responds to the shadow wake (the source of greatest dynamic excitation), the neighboring blade fails to respond significantly, i.e., the blade in clean air maintains a particular response trajectory regardless of its root loads. Hence, both blade shanks share the deflection required by the response of the blade leaving the shadow region, reducing the loads in both shanks by one half.

Mod 0 system, between the blade root flanges and the hub. All four devices are essentially flexures that reside substantially inside of the existing Mod 0 blade and cuff assemblies. As such, they add only 15.2 centimeters (.5 feet) to the Mod 0 rotor radius.

Two of the flexures are steel and two are unidirectional fiberglass. Table VIII presents key design and loads data associated with these designs, indicating that the fiberglass units are superior, particularly from a fatigue standpoint.

One of the fiberglass flexures is symmetrical, having equal stiffness in all directions of bending. The rectangular section has been arranged for more stiffness in the plane of rotation than out of the plane. The unfortunate fact that the blade feathering hinge is inboard the flexures, however, means that the flexure principal axes rotate with respect to the rotational plane, with rotor feathering. Feathering angle is, of course, a function of wind and rotor speed, and power level.

Analysis of the Flexures - An analysis was performed to determine the modeshapes and frequencies of the blade/flexure combination, as a function of flexure design and feathering angle. These results were then input to MOSTAB-HFW, to solve for the resulting blade loads and motions. Figures 29 through 31 show key MOSTAB-HFW results applicable to the symmetric and asymmetric fiberglass flexure designs depicted by Figures 25 through 28. A few conclusions that can be derived from these analysis results are:

- a) Flapwise bending loads are reduced by the relatively soft flexures, by 50 percent for the symmetric flexure and 60 percent for the asymmetric flexures.
- b) Because of the low inplane natural frequencies of the symmetric and asymmetric flexures (1.5 P and 1.91 P, respectively) compared to the stiff Mod 0 inplane support (3.6 P), the dynamic inplane loads are seriously aggravated by the flexures. The one-per-rev gravity loads and the dynamic amplification associated with this 1 P load, acting closer to resonance than in the baseline Mod 0 system, is undoubtedly responsible for these increased loads.
- c) As might be expected, the asymmetric flexure with its higher inplane frequency has improved inplane loads over those developed by the symmetric flexure.
- d) Because the soft flexures cannot maintain precone, as is possible with the teetering design, gusts or operation at full speed and low power levels can be expected to "uncone" the rotor into the tower. Hence, the flexure concept will generally require more blade/tower clearance than the teetering concept, probably to the point of requiring a shaft tilt to swing the blades well clear of the tower.

As was the case with the teetering analysis, the coupled analysis computer code was not available for the flexure device examinations. All these studies were conducted with the fixed-shaft and constant rotor speed assumptions.

General Conclusions - Articulation Devices

The teetering articulation can be expected to reduce blade flapwise loads by roughly half for systems with very stiff shaft supports; with softer systems, such as the baseline Mod 0 design, the loads reduction can be expected to be less. In the case of the Mod 0 system, a teetering rotor can reduce flap loads by about 30 percent, with relatively minor impact on inplane loads. Since the teetering concept retains precone, it does not tend to aggravate tower clearance margins, although certain types of gusts can be expected to teeter the rotor into the tower.

The flexure devices offer the most potential for reducing flapwise loads, but a high inplane stiffness is required to avoid paying a severe attendant penalty in inplane loading. The problem of maintaining a small ratio between flap and inplane flexural bending stiffnesses is exacerbated by the location of the feathering hinge inboard of the flexures. Because the flexures are soft, the wind turbine rotor shaft should be tilted if they are incorporated, to provide ample blade/tower clearance.

It should be noted that rigid rotor blades are all essentially flexures, with the flexural elements integral with the blade. Future wind turbine blade design activities should address the concept of making the flap stiffnesses lower, while maintaining a high inplane stiffness, to achieve the benefit of the soft flexure on flap loads without the penalty on inplane loads. Also, the softer (flapping) blades will require more tower clearance, not so much because of dynamic flapping, but because of static coning.

DISCUSSION OF RESULTS

Because the subject contractual activity has been executed in distinct subactivities, the discussions of results appear in previous sections of this report.

Results associated with the Mod 0 articulation concepts were presented in the section entitled, "Design and Analysis of Candidate Mod 0 Hub Articulation Concepts."

CONCLUSIONS AND RECOMMENDATIONS FOR FURTHER RESEARCH

A complete coupled analysis software system has been developed for application to a broad range of wind energy machine designs. The system addresses wind machine dynamics in both the frequency and the time domains, and includes the interactions of the rotor, nacelle, power train, control system and electrical equipment.

Based on the current status of the work supported by the subject contract, a number of additional developments can be recommended which would enhance the accuracy and utility of the wind energy system coupled dynamics analysis. A few of these are presented below.

Verification of MOSTAS

The fundamental purpose of the subject contractual work was the development of the wind energy system coupled dynamics code, MOSTAS. Example MOSTAS executions, presented in Reference 3, were prepared for check cases, to be run when MOSTAS is brought up on a given computer system. The examples, configured specifically to check the code, are not satisfactory for analysis system verification.

Accordingly, a very important future step in the MOSTAS development process would be verification of computed results by comparison with available test data. It is anticipated that such comparisons will be made, using Mod 0 test data, in the very near future.

Improved Accuracy

The section entitled "Component Model Descriptions" identified procedures for rigorous treatment of the time-varying constituents in the coupled dynamics equation operators. These include Floquet* analysis for the frequency-domain examinations and advanced numerical integration procedures for the time domain analysis. It is highly recommended that these advanced procedures be incorporated in the code.

Some key areas of the dynamic analysis code should be typed double precision, particularly if they are to handle large systems.

* Paragon Pacific, Inc. has a procedure called the "Root Perturbation Method," which is expected to yield the Floquet roots of large periodic systems without the usual numerical problems associated with Floquet analysis. Upon development, this new method should be implemented in the wind energy system analysis.

Select Nonlinearities

The coupled system code is capable of solving for dynamic responses with the presence of key system nonlinearities such as gear backlash, control system linkage hysteresis and power train nonlinear damping and flexibilities. In the event that such analysis results are needed to support the development of wind power machines, MOSTAS should be extended to include the nonlinearities of interest.

Utility Items

A number of convenience items might be added to the coupled system analysis, considerably enhancing its utility. A few items in this category are:

- a) Plot packages;
- b) Input data check codes, examining the boundaries of user-specified data for compatibility with available storage allocation, and other program constraints;
- c) Miscellaneous improved and extended print formats.

In addition to the recommendations forwarded above for the dynamic analysis software, it is recommended that the key conclusions reached during the hub articulation design and analysis activities be re-examined using the full coupled system analysis in lieu of the basic fixed-shaft analysis methods.

Lewis Research Center
National Aeronautics and Space Administration
Cleveland, Ohio 44135
January, 1977

REFERENCES

1. Henninger, William C.; Hoffman, John A.; and Williamson, Dale R.: Mathematical Methods Incorporated in the Wind Energy System Coupled Dynamics Analysis: Part I - Basic Methodology for the Modular Stability Derivative Program (Revision B); Part II - Analysis Methods Incorporated in the MOSTAB-HFW Computer Code; Part III - Methodology: Wind Turbine Linear Analysis Software System (WINDLASS). PPI-1014-7, Paragon Pacific, Inc., January, 1977.
2. Henninger, William C.; and Hoffman, John A.: Analysis Methods Incorporated in the Rotor Linear Modelling Program (ROLIM), PPI-2001-2, Paragon Pacific, Inc., October, 1976.
3. Henninger, William C.; Hoffman, John A.; and Williamson, Dale R.: MOSTAS User's Manual: Volume I - User's Manual for the Modular Stability Derivative Program - High Frequency Wind Turbine Version (MOSTAB-HFW), PPI-1014-8; Volume II - User's Manual for the Wind Turbine Linear Analysis Software System (WINDLASS), PPI-1014-9. Paragon Pacific, Inc., January, 1977.
4. Hoffman, John A.: Wind Turbine Analysis Using the MOSTAB Computer Program. MRI Report 2690-1, Mechanics Research, Inc., 1974.
5. Janetzke, D. C.; Puthoff, R. L.; and Richards, T. R.: Rotor Performance Predictions for the LOOKW Experimental Wind Turbine. Preliminary report, NASA Lewis Research Center.
6. Spera, David A.: Structural Analysis of Wind Turbine Rotors for NSF-NASA Mod-0 Wind Power System. NASA TM X-3198, 1975.
7. Williamson, Dale R.: Design of Articulated Hub Concepts (Final Report): Volume I - Teetering; Volume II - Flexures, PPI-1014-10. Paragon Pacific, Inc., January, 1977.
8. Hohenemser, Kurt H.; and Sheng-Kuang Yin: Some Applications of the Method of Multiblade Coordinates. Journal of the American Helicopter Society, vol. 17, no. 3, July, 1972.
9. Hoffman, John A.: Some Practical Aspects Associated with Digital Execution of Rotorcraft Math Models for Time-Domain Simulation. PPI-3010, Paragon Pacific, Inc., November, 1976.
10. Hurty, Walter C.; and Rubinstein, Moshe F.: Dynamics of Structures. Prentice-Hall, Inc., 1964.
11. Glasgow, J. C. (5252/Wind Power Office): Memorandum to Wind Turbine Dynamics Review Committee; Subject - Selected Mod-0 Experimental Wind Turbine Operational Data (unpublished). NASA Lewis Research Center, Cleveland, Ohio, March 4, 1976.

TABLE 1. - HISTORY OF MOSTAB/ROLIM SYSTEMS

TIME	PROJECT	SUPPORT
1965-69	DEVELOPMENT OF ROTOR MATH MODELS; DIGITAL AND ANALOG SIMULATION (ORIGINAL REXOR CODES)	LOCKHEED IRAD
1969-72	ORIGINAL MOSTAB DEVELOPMENT FOR ROTORCRAFT ANALYSIS; MOSTAB-B, MOSTAB-C, MOSTAB-CR AND MOSTAB-HIV VERSIONS; CODES PUBLISHED AND PUBLIC DOMAIN	U.S. ARMY (EUSTIS) NASA (LANGLEY)
1972-74	MOSTAB VERSIONS EXPANDED FOR BLOWN ROTOR AND AEROELASTIC ANALYSIS MOSTAB-CCR (CIRCULATION-CONTROLLED ROTOR) MOSTAB-HFA (HIGH FREQUENCY ANALYSIS)	U.S. NAVY (NAVAIR MONITORED BY DTNSRDC)
1973-74	BASIC MOSTAB-CR REFINED FOR WT ANALYSIS	NASA (LEWIS)
1974-75	ROTOR LINEAR MODELLING CODE (ROLIM) DEVELOPED	PARAGON PACIFIC IRAD
1975 TO DATE	MOSTAB-HFA EXTENDED TO MOSTAB-HFW FOR COUPLED WT ANALYSIS	NASA (LEWIS)
1975 TO DATE	MOSTAB-HFA EXTENDED FOR X-WING ANALYSIS	U.S. NAVY

TABLE II. - DATA INTERFACES BY SUBCODE; WIND ENERGY SYSTEM
COUPLED DYNAMICS ANALYSIS

SUBCODE: DATAIN

Input Data Required

Basic MOSTAB input data from cards:

1. Physical features of each component -

Earth: Effective aerodynamic area and drag coefficient

Tower: Effective aerodynamic area and drag coefficient

- Rotor:
- Miscellaneous indices describing numerical sector sizes
 - Nominal speed
 - Radius
 - Angular orientation with respect to other wind machine elements
 - Radial schedules, geometry
 - chord
 - twist
 - coning shape
 - Radial schedules, mass properties
 - distributed mass
 - center of gravity location
 - blade-section inertia tensor
 - Radial schedules, dynamic properties, modeshapes
 - Frequencies for each blade mode
 - Numerical integration procedure for each blade mode
 - Gimbal properties, if applicable (gimbal type, undersling distance and teeter/pitch coupling)

2. Relative locations of each component in the overall system

3. Aerodynamic interference model properties -

Wake properties

Wake coupling coefficients

Shadow wake profile definition

4. Operational conditions -

Wind speed

Air properties (density, temperature, etc.)

Rotor precession rates

TABLE II. - Continued

5. Miscellaneous numerical indices (numerical differentiation increments, etc.)

Output Data Produced

1. Formatted printed input data (line printer)
2. Unformatted binary data file for input to MOSTAB (sequential access disk or tape file)

SUBCODE: MOSTAB-HFW

Input Data Required

1. Data file unit definition and executive option flag (card)
2. Binary file produced by subcode DATAIN (disk or tape)

Output Data Produced (Line Printer)

1. Essential constant data for rotor analysis: generalized masses, completed modeshape functions, etc.
2. Results of successive trim-search passes
3. Results of successful trim search -
Rotor average shaft loads produced for trim (resolved to a nonrotating coordinate system)
Wake velocity components (e.g., retardation velocities) developed at trim
Average power produced
4. Gradient arrays showing rotor shaft load responses to variations in relative wind speed components, shaft precession rates and rotor control variations.

Output Data Produced (PROCES File - Sequential Access Tape or Disk)

1. Rotor blade motion data at trim - blade modal coordinates and their time derivatives as a function of blade azimuth.

TABLE II. - Continued

2. Gimbal degrees of freedom, motions and their time derivatives vs. azimuth (if applicable).
3. Rotor blade internal loads vs. radius and azimuth
4. Shaft loads produced by one blade vs. azimuth
5. Aerodynamic distributed loads data vs. radius and azimuth, including angle of attack, mach number, dynamic pressure, lift, drag and moment coefficients, and distributed force and moment air loads.

Output Data Produced (ROLIMX File - Sequential Access Tape or Disk)

1. Basic geometric and trim-search data -
Relative geometric location of elements in wind turbine system
Mass properties of rigid body mass elements associated with system
Trim-search loads results
2. Linear math model for a single rotor blade -
Shaft loads
Gimbal error function (if applicable)
Generalized forcing function applied to blade modes

These linear math models appear as gradient arrays operating on all blade and shaft degrees of freedom and on control and rotor speed input functions, and their time derivatives. The gradient arrays are functions of azimuth.
3. Linear math models representing the aerodynamic couplings among the aerodynamic elements of the wind turbine system

SUBCODE: PROCES

Input Data Required

1. Data file unit numbers and executive option indices (card)
2. PROCES data file produced by MOSTAB-HFW (see MOSTAB-HFW, output data produced: PROCES data file, above)

TABLE II. - Continued

Output Data Produced (Line Printer)

1. Formatted printout of the basic trim loads and motion data on the PROCES input data file
2. Internal blade loads and shaft loads produced by a single blade, by frequency component (harmonic analysis results performed by PROCES)

Output Data Produced (Card Punch - Optional)

Harmonic blade and shaft loads

SUBCODE: ROLIM

Input Data Required

1. Data file unit numbers, executive option indices, and harmonic and time-point specifications on ROLIM output data (card)
2. ROLIMX data file produced by MOSTAB-HFW (see Subcode: MOSTAB-HFW, Output Data Produced, above)

Output Data Produced (Line Printer and Sequential Access Tape
or Disk File)

Linear math model of rotor system, including all blades aerodynamically coupled (and mechanically coupled in the case of gimbaled rotor analysis)

1. Model arrays operating on rotating coordinates and expressed as a function of azimuth position
2. Same as 1., except expressed as sine/cosine Fourier coefficients
3. Same as 2., except expressed as amplitude/phase angle Fourier entities
4. Model arrays transformed to operate on multi-blade coordinates - models have reduced one-per-rev components - expressed as functions of blade azimuth position
5. Same as 4., except expressed in sine/cosine Fourier coefficients

TABLE II. - Continued

6. Same as 5., except expressed in amplitude/phase angle Fourier entities

SUBCODE: COUPLED DYNAMIC SYSTEM LINEAR ANALYSIS (WINDLASS)

Input Data Required (Tape or Disk File)

Type 4 output data produced by ROLIM: linear rotor math model, operating on multi-blade coordinates and expressed in sine/cosine coefficient form (tape or disk file)

Input Data Required (Cards)

1. Data file unit definition and executive option flags
2. Executive specification indices which define, by code -
 Input data items
 Independent variables to be included in the coupled system dynamic equation
 Dependent variables associated with the coupled system dynamic equations
 Variables defined as "removable"; i.e., variables included in the elemental formulations of the linear math models which are to be ultimately calculated, but which can be eliminated from the basic coupled system dynamic equation
 Miscellaneous other executive specification indices
3. Physical data associated with each component of the wind energy system, excluding the rotor -
 Tower: Modeshapes, frequencies and mass properties; base flexibilities, inertia and damping properties; dimensional geometry
 Power
 Train: Inertia, stiffness, damping and gear ratio coefficient associated with each "building block" in the power train; specification indices which link the power train building blocks

TABLE II. - Concluded

Control

System: (Model includes dynamic characteristics of power machinery, power machinery controls, power generating reflected torques and network elements) -
Loop specifications, transfer functions and gains

Pod: (Nacelle) - Stiffness and inertia properties;
geometry at rotor, tower and power train interface
locations

4. Harmonic coefficients required to define dynamic shaft and blade loads, produced by subcode PROCES.

Output Data Produced (Line Printer)

1. Linear operators in coupled system dynamic equation
2. Linear operators in "removable" variable equation (solvable from results of coupled system dynamic equation)
3. Eigenvalues and eigenvectors (reflecting coupled system stability) computed from the homogeneous portion of the dynamic equation
4. Time-history responses of selected system independent and removable variables, representing the coupled system perturbation responses from the trim condition responses calculated by MOSTAB-HFW
5. Time-history responses, periodic blade root loads: superposition of trim loads computed by MOSTAB-HFW and perturbation coupled dynamic loads

TABLE III. - METHODS OF DYNAMIC ANALYSIS -- ROTOR SYSTEMS

ADVANTAGES		DISADVANTAGES	
TIME-DOMAIN SIMULATION			
<ul style="list-style-type: none">● MANY DOF AND NONLINEARITIES● FLEXIBLE PROGRAMMABILITY		<ul style="list-style-type: none">● EXCESSIVE COMPUTER COSTS● CONSTANT RE-SOLUTION● DIFFICULT STABILITY EVALUATIONS● NUMERICAL INSTABILITY HAZARD	
FREQUENCY-DOMAIN SOLUTION STANDARD PROCEDURES			
<ul style="list-style-type: none">● CLEAR STABILITY EVALUATION● COMPONENT MODELS		<ul style="list-style-type: none">● CONSTANT COEFFICIENTS REQUIRED● QUASI-STATIC ASSUMPTION	
MOSTAB/ROLIM SYSTEM			
<ul style="list-style-type: none">● ALL ADVANTAGES OF FREQUENCY-DOMAIN STABILITY ANALYSIS - LINEAR ANALYSIS● PERIODIC MATH MODELS● HIGH FREQUENCY ROTOR MODES		<ul style="list-style-type: none">● REQUIRES FLOQUET OR ROOT-PERTURBATION METHOD ANALYSIS	

TABLE IV. - VECTORS FOR WIND TURBINE COUPLED SYSTEM

Symbol	Description ^a
c, \dot{c}, \ddot{c}	Control system inputs to rotor. (NC)
f	Perturbation load on rotor due to freeing fixed shaft. (6)
f_{EP}	External load applied to pod. (NP6)
f'_{EPR}	Load at pod/rotor interface point, applied to pod. (6)
f_{EPT}	Load at pod/tower interface point due to elastic deformation of pod. (6)
f_{ET}	External loads applied to tower. (NT6)
f_H	Total load on moving hub, at rotor/pod interface point. (6)
f_{TP}	Load at pod/tower interface point applied to tower. (6)
f_O	Fixed shaft load applied to hub mass - from MOSTAB-HFW: (6)
f'_O	Total moving shaft load applied to hub mass. (6)
h, \dot{h}	External inputs to control system. (NH)
x, \dot{x}, \ddot{x}	Rotor shaft perturbation motion. (6)
x_P	Pod grid point displacements. (NP6)
x_T, \ddot{x}_T	Displacement, acceleration of tower grid points. (NT6)
x_{TP}, \ddot{x}_{TP}	Displacement, acceleration of tower/pod interface point. (6)
y	Rotor degrees of freedom. (NY)
α	Control system degrees of freedom. (NA)
γ_B	Power train gear box reaction torque, applied to pod. (NBOX)
γ_C	Control system torque applied to power train. (1)
γ_{CP}	Control system torque applied to pod. (NGCP)

^aItems in parentheses are vector length (see Table VI).

TABLE IV. - Concluded

Symbol	Description
γ_{EP}	External torque applied to power train. (NPHI)
γ_{RPT}	Power train torque applied to rotating hub mass. (1)
δ	Tower base degrees of freedom. (3 or 6)
ξ	Tower modal coordinates. (NEV)
φ	Power train independent degrees of freedom (NPHI)
$\varphi_{RPT}, \dot{\varphi}_{RPT}, \ddot{\varphi}_{RPT}$	Rotor rotation, speed and acceleration perturbations. (1)
ψ	Rotor azimuth angle. (1)
$\Omega, \dot{\Omega}$	Rotor speed and acceleration perturbations. (1)

TABLE V. - OPERATORS FOR WIND TURBINE COUPLED SYSTEM

Symbol	Description
$A_{\alpha}, \dot{A}_{\alpha}$	Control system operators
$B_B, B_{EQ}, B_N,$ B_P, B_R, B_{ϕ}	Damping operators for power train equations
B_h, \dot{B}_h	Control system operators for external input, h
$B_y, \dot{B}_y, \ddot{B}_y$	Control system operators for rotor degrees of freedom, y
$B_{\Omega}, \dot{B}_{\Omega}$	Control system operators for rotor velocity and acceleration $\Omega, \dot{\Omega}$
$D_{\alpha}, \ddot{D}_{\alpha}$	Relate control system degrees of freedom to rotor control variables
E_{CP}	Rotational transformation and partitioning operator for control system torques applied to pod
E_{EX}	Rotational transformation matrices for externally applied pod loads
E_{PR}	Rotational transformation operator for pod loads at the rotor/pod interface point
E_{PPT}	Rotational transformation and partitioning operator for power train gear box torques applied to pod
E_{TP}	Rotational transformation matrix to express tower loads and deflections in the pod reference system
E_{XPR}	Rotational transformation and partitioning operator for pod deflections at the rotor/pod interface point
E_{α}	Relates control system degrees of freedom to generator torque
F_T	Tower modal force participation factor for external tower loads
F_I	Tower modal force participation factor and partitioning operator for load at tower/pod interface point

TABLE V. - Continued

Symbol	Description
G	Tower grid point geometric operator for external tower loads
G_I	Tower grid point geometry and partitioning operator for load at tower/pod interface point
G_T	Tower grid point geometric operator for external tower loads
I_C	Partitions generator torque γ_C reaction to appropriate gear box
I_{EP}	Partitions main gear torques to power train dofs
I_{EPT}	Applies the pod/tower interface load to the appropriate pod degrees of freedom
I_{PF}	Partitions reactions applied by the rotor to the pod
I_{PT}	Partitions out those pod degrees of freedom at the pod/tower interface point
I_{XO}	Partitions fixed shaft loads f_0 to rotor/pod interface point
I'_{XO}	Partitions fixed shaft torque from f_0 to power train.
I_{XT}	Partitioning operator for motion of tower/pod interface point
I_{XX}	Partitions out the five rotor shaft displacements that are compatible with the pod
I_Y, I_Y^*	Partitioning operators for moving shaft degrees of freedom
$J_B, J_{EQ}, J_N,$ J_P, J_R, J_ϕ	Inertia operators for power train equations
J'	Effective inertia of tower base, including mass loading by tower
J_H	Rotor polar moment of inertia

TABLE V. - Continued

Symbol	Description
J_X	Partitioned rotor polar moment of inertia
K	Power train shaft torsional stiffness operator, or tower base stiffness operator
$K_B, K_{EQ}, K_N,$ K_P, K_R, K_ϕ	Stiffness operators for power train equations
K_P	Pod stiffness operator or power train stiffness operator
K_O	Differential stiffness operator for fixed shaft load in moving hub coordinate system
M	Rotor acceleration operator, from ROLIM
M_H	Non-spinning rotor hub mass matrix
M_{PE}	Pod mass matrix, transferred to tower/pod interface point
M_δ	Tower grid point mass loading on tower modes
M_ξ	Tower modal mass loading on tower base
P	Rotor velocity operator, from ROLIM
P_α	Relates control system response to torques on the pod
Q	Rotor displacement operator, from ROLIM
R_c, R_c^*, R_c^{**}	ROLIM operators for applying control inputs to rotor
R_f	ROLIM operator for applied rotor shaft load
R_Ω, R_Ω^*	ROLIM operators for changes in rotor speed and acceleration
U	Unity 6 x 6 operator
U_B	Unity operator for power train gear box torque reactions

TABLE V. - Concluded

Symbol	Description
U_c	Unity operator for rotor controls, c , \dot{c} and \ddot{c}
U_{CP}	Unity operator for control system torque reaction to pod, γ_{CP}
U_T	Unity operator for tower degrees of freedom
U_ξ	Unity operator for tower modal degrees of freedom
U_1	Unity 1 x 1 operator
W	Tower modal frequency operator
X_ξ	Tower mode shapes, fixed base

TABLE VI. - VECTOR LENGTHS FOR WIND TURBINE COUPLED SYSTEM

Symbol	Description
NA	Control system degrees of freedom
NB	Tower base degrees of freedom (3 or 6)
NBOX	Power train gear boxes
NC	Rotor control degrees of freedom
NEV	Eigenvalues in tower modal model
NGCP	Interface degrees of freedom between pod and control system
NH	External inputs to control system
NPHI	Power train gear block elements and independent degrees of freedom
NP6	Pod degrees of freedom (6 times the number of grids)
NT6	Tower degrees of freedom (6 times the number of grids)
NY	ROLIM rotor model degrees of freedom

TABLE VII. - TEETERING HUB DESIGN CONCEPTS - WEIGHTS AND OTHER DESIGN DATA

Teetering Concept	Weight ^a (N)	Outboard Shift of Hub (m)	Undersling (m)	Stop Mechanism	Description	Comments
Long Yoke	15,100	0.178	0.478	Hydraulic Cylinders	Long yoke places teetering axis near overall c.g.	Requires modified outboard hub plate; heaviest concept
Short Yoke	9,800	0.178	-0.386	Hydraulic Cylinders	Short yoke places teetering axis near shaft face, for minimum weight	Negative under- sling is unconventional
Linkage	10,200	0.381	0.914	Hydraulic Cylinders	Basic four-bar linkage places teetering axis at classical under- slung location	Least conventional; teetering axis translates slightly as linkage moves

^a Stop mechanism not included

TABLE VIII. - BLADE ROOT FLEXURES - SUMMARY

DESIGN	A Steel Unsymmetric	B Steel Symmetric	C Fiberglass Unsymmetric	D Fiberglass Symmetric
Material	4340 Steel HT to $1.1 \times 10^9 \text{ N/m}^2$		Unidirectional Fiberglass	
Modulus of Elasticity (10^{-10} N/m^2)	21	21	3.9	3.9
Dimensions (m)*074x.147x1.46	.12 dia x 1.52	.10x.198x.91	.16 dia x .91
Flexure Weight (N /blade)	1748	1792	578	578
Total Assembly Weight (N /blade)	6227	6227	4581	4581
Divergence Speed, m/sec from T.E. @ 45 degrees	47.4	60.8	45.6	58.1
Inplane Natural Frequency (per-rev at $\Omega = 4.2 \text{ rad/sec}$)	1.91P	1.50P	1.91P	1.50P
Inplane Bending Moment Range** ($\text{N} \cdot \text{m} \times 10^{-3}$)	+77 to -85	+81 to -119	+34 to -85	+81 to -119
Maximum Flexure Inplane Stress ($\text{N/m}^2 \times 10^{-8}$)	3.24	6.9	1.31	2.96
Flapwise Natural Frequency (per-rev at $\Omega = 4.2 \text{ rad/sec}$)	1.50P	1.91P	1.50P	1.91P
Maximum Flapwise Bending Moment ($\text{N} \cdot \text{m} \times 10^{-3}$)	51.5	89.5	51.5	89.5
Flapwise Bending Moment Reduction ***	67%	43%	67%	43%
Maximum Flexure Flapwise Stress ($\text{N/m}^2 \times 10^{-8}$)	3.93	5.31	1.59	2.21
Maximum Deflection When Passing Tower (m)	0.98	0.67	0.98	0.67
Deflection Increase ****	39%	-4%	39%	-4%
Zero Load Steady Cone [†] (angle from vertical)	4 degrees	5 degrees	4 degrees	5 degrees

* Preliminary - Dimensional revisions (to stiffen) are required to achieve 1.5P lowest frequency.

** Over MOSTAB prediction for current Mod-0, rigid shaft (Figure 4.3, Reference 8).

*** Rigid Shaft Mod-0 prediction is +34 to -85 $\text{N} \cdot \text{m} \times 10^{-3}$ (Figure 4.4, Reference 8).

**** Rigid Shaft Mod-0 prediction is 0.7 m at $\psi = 10$ degrees (Figure 4.5, Reference 8).

[†] Assumes 7 degrees precone; zero load steady cone for current Mod-0 = 6 degrees from vertical.

FIGURE 1. - COUPLED DYNAMICS ANALYSIS (MOSTAS)
- GLOBAL ARRANGEMENT.

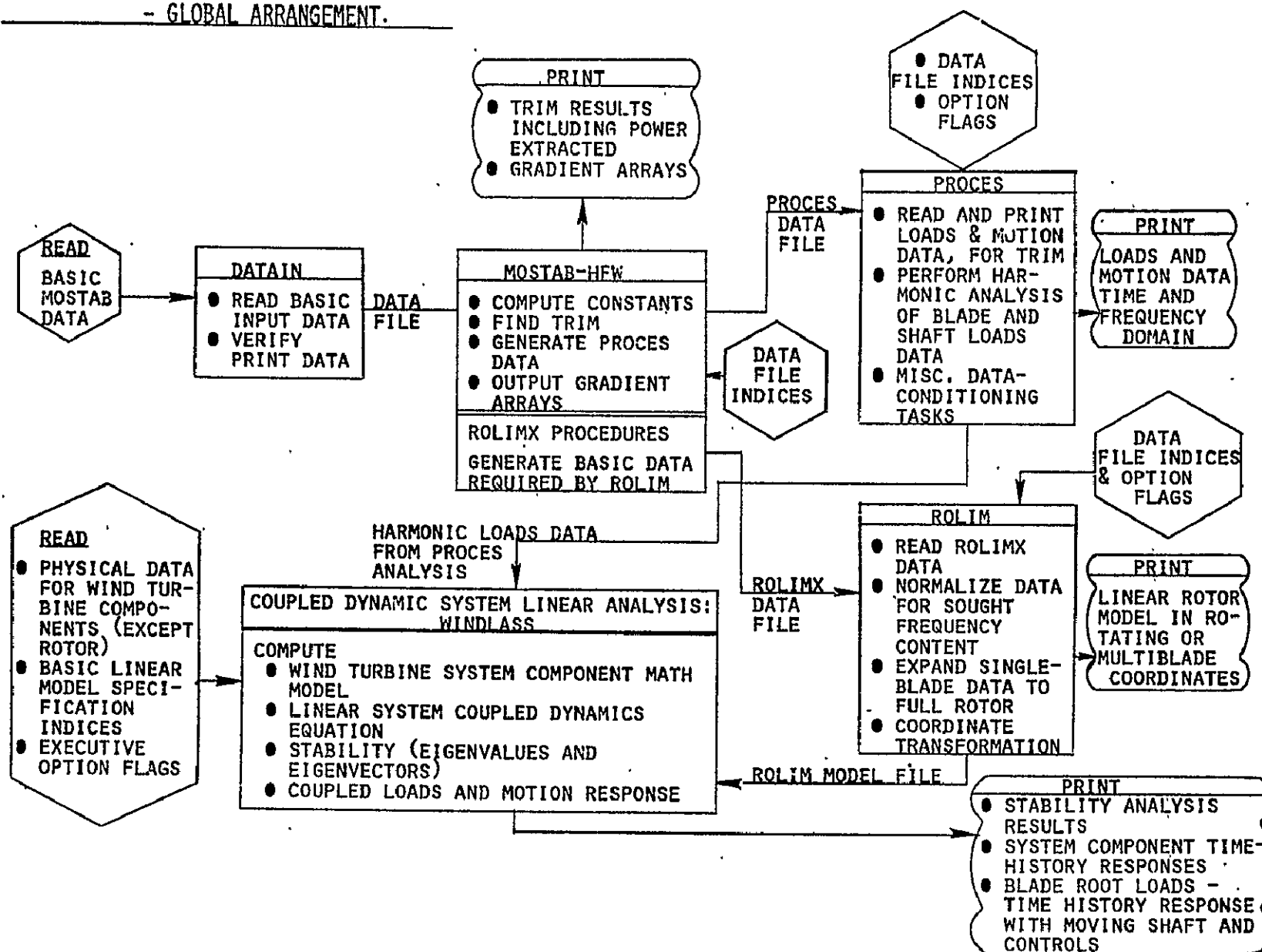
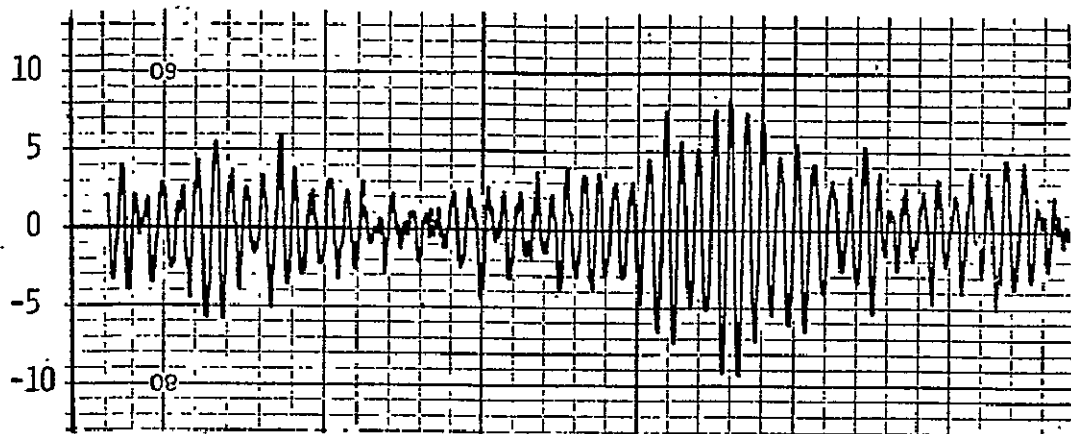
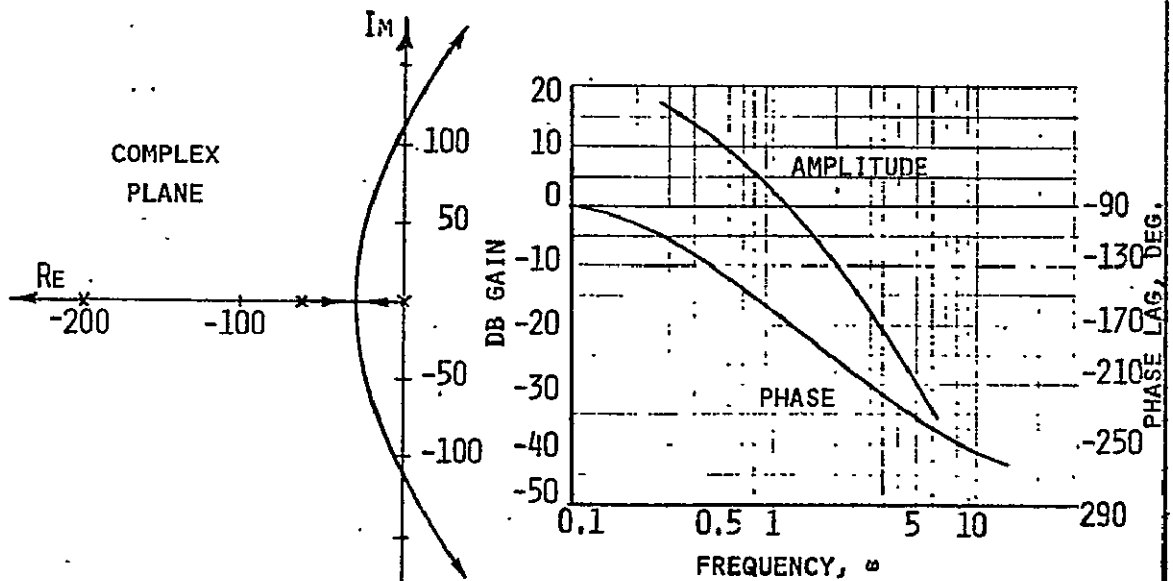


FIGURE 2. - TIME AND FREQUENCY DOMAIN ANALYSIS METHODS.

STABILITY ANALYSIS METHODS



TIME DOMAIN



ROOT LOCUS PLOT

BODE PLOT

FREQUENCY DOMAIN

FIGURE 3. - BASIC MOSTAB/ROLIM ANALYSIS PROCEDURES.

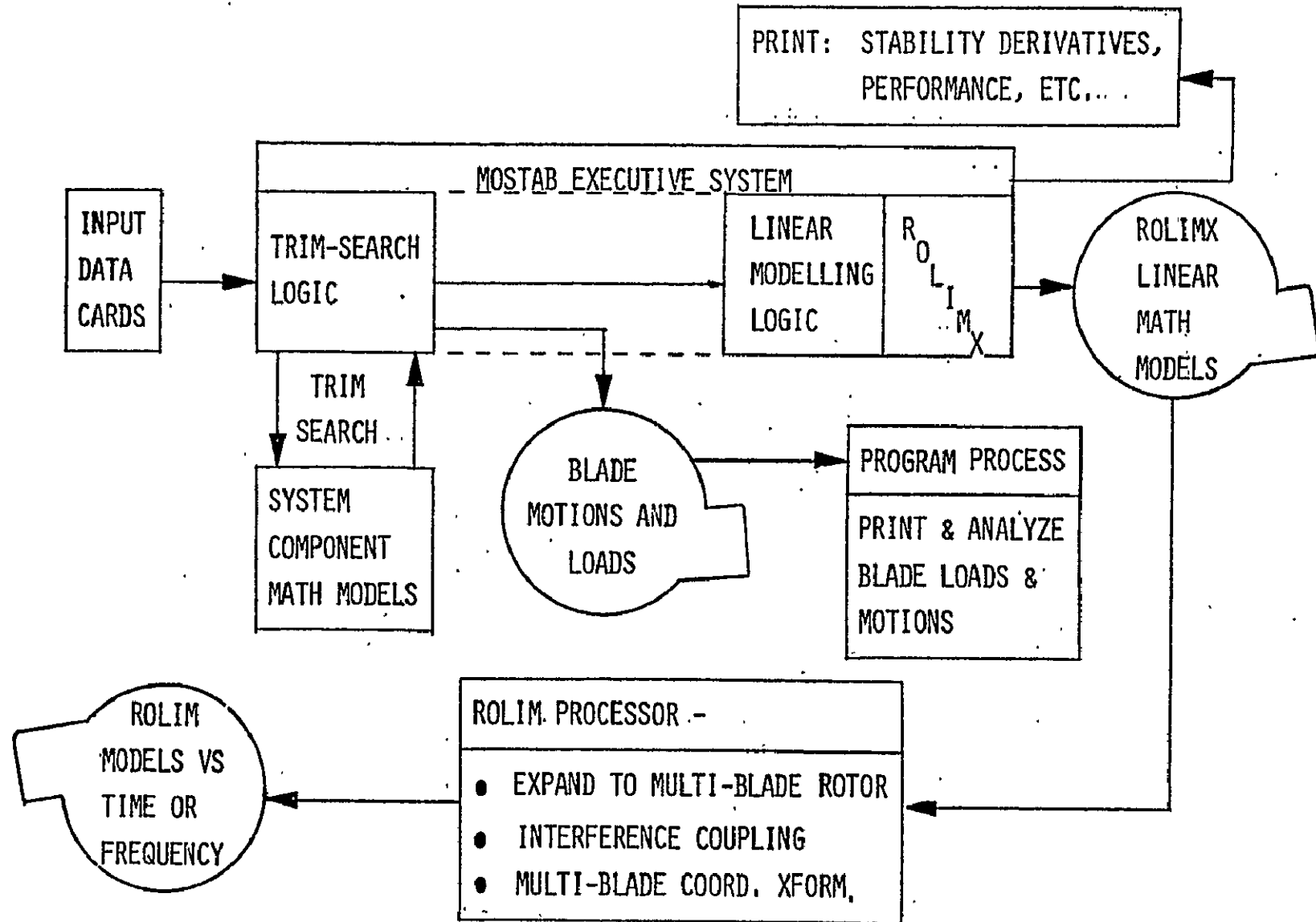


FIGURE 4. - ESSENTIAL ELEMENTS OF MOSTAB MATH MODELS.

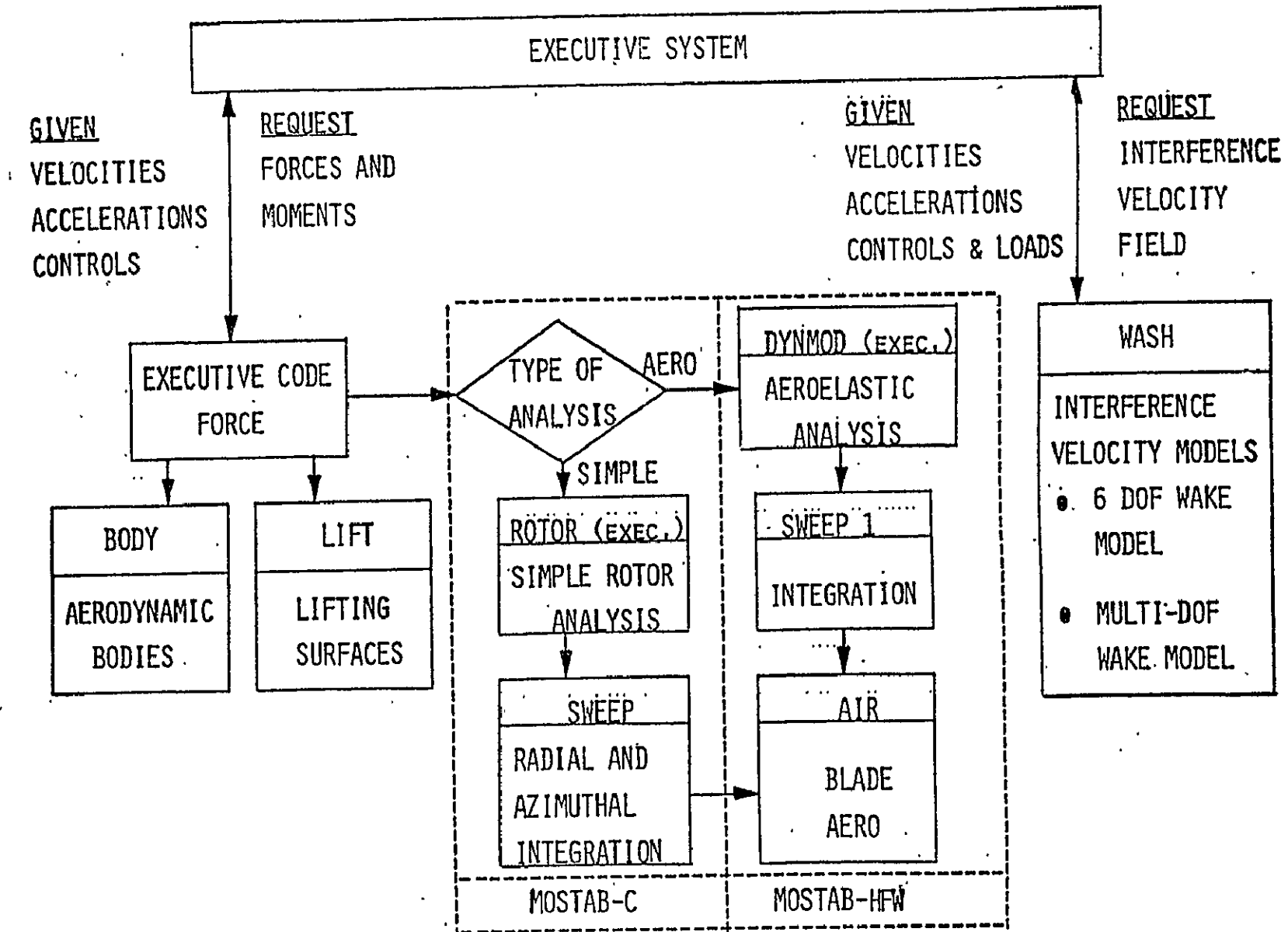


FIGURE 5. - MOSTAB EXECUTIVE LOGICAL PROCEDURE.

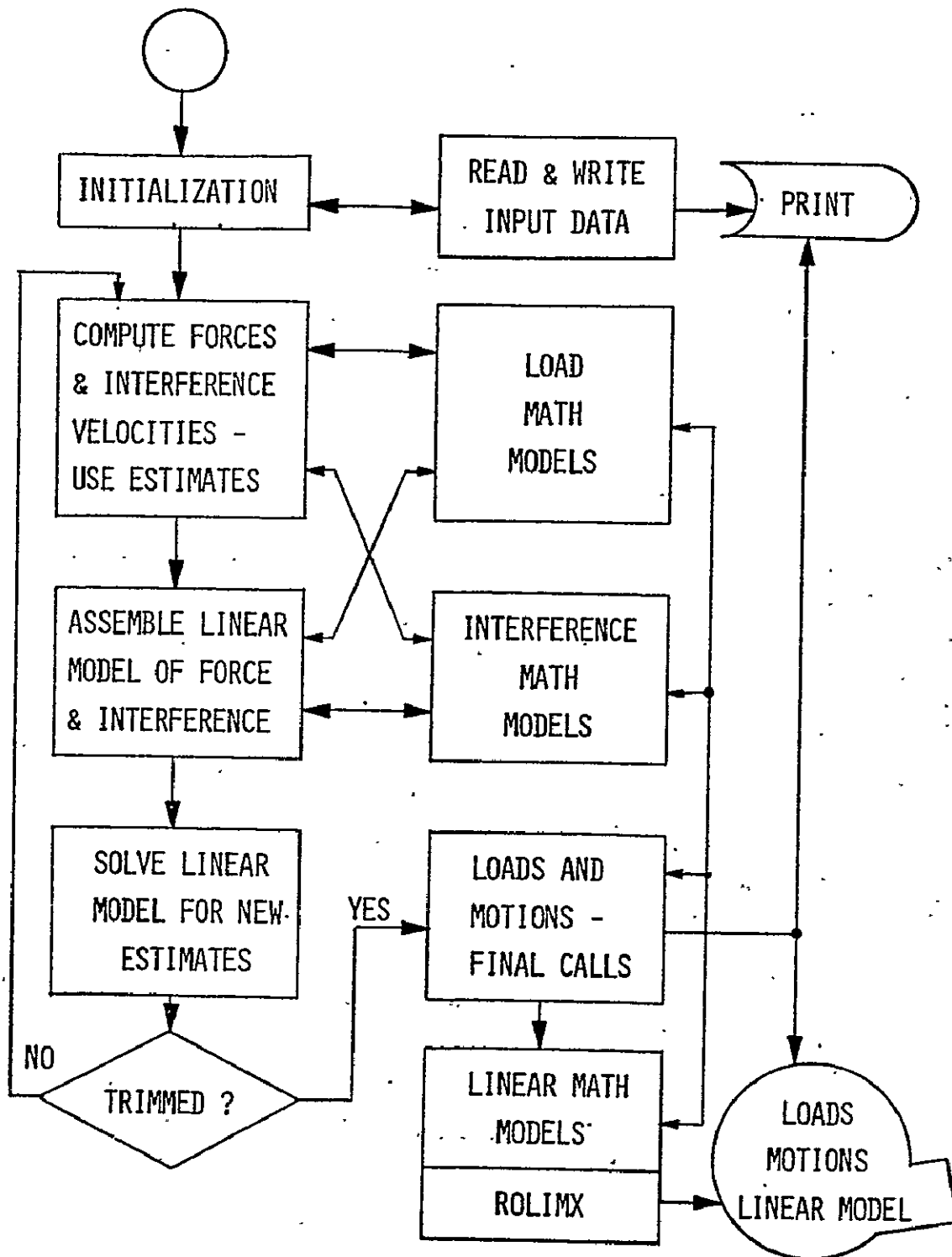
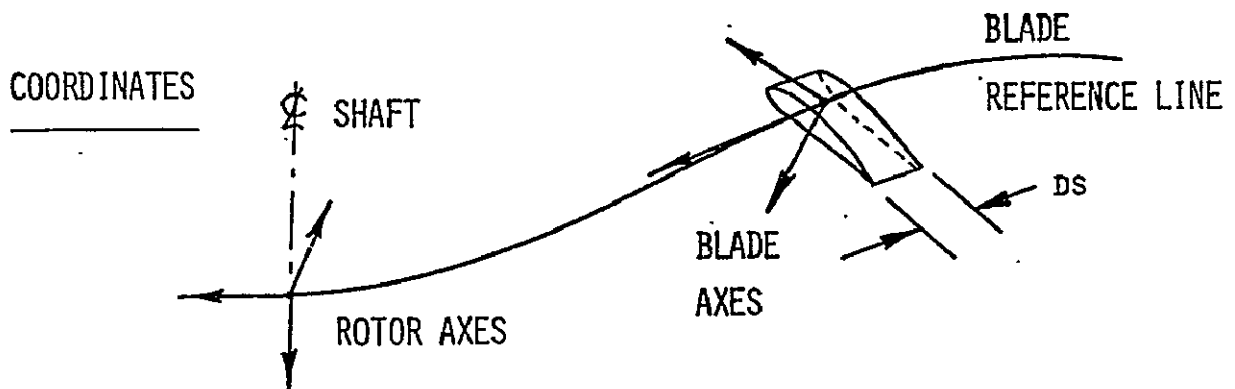


FIGURE 6. - FUNDAMENTALS OF ROTOR ANALYSIS.



ATTRIBUTES

SIMPLE ROTOR ANALYSIS

- ONE DOF, CONSTRAINED TO MOTION PARALLEL TO SHAFT
- BLADE ELEMENT A POINT MASS

AEROELASTIC ANALYSIS

- USER-SPECIFIED NUMBER OF DOF
- BLADE ELEMENT MASS AND INERTIA TENSOR
- SIX-DOF ELEMENTAL MODEL

BOTH

STATIC AERO-STALL AND COMPRESSIBILITY;
FUNCTION OR TABLE-LOOK UP

FIGURE 7. - AEROELASTIC BLADE ANALYSIS.

SINGLE BLADE MODEL, ISOLATED BY
SHAFT WITH PRESCRIBED MOTION

BLADE ELEMENTS MOVE IN SIX DOF

MODAL MODEL TRANSFORMS BLADE
MOTION TO NORMAL COORDINATES

MODEL REQUIRES INPUT

- MODESHAPES (6 DOF)
- FREQUENCIES
- INERTIAL PROPERTIES
- NUMBER OF DOF
- INITIAL SHAPE

BLADE-MODE INITIAL CONDITIONS DETERMINED
BY ITERATIVE PROCEDURE

GIMBAL ANALYSIS USES ITERATIVE PROCEDURE
AND SINGLE-BLADE MATH MODEL

FIGURE 8. - GIMBAL ANALYSIS,

GIVEN: SHAFT AND AIR
MOTIONS, CONTROL

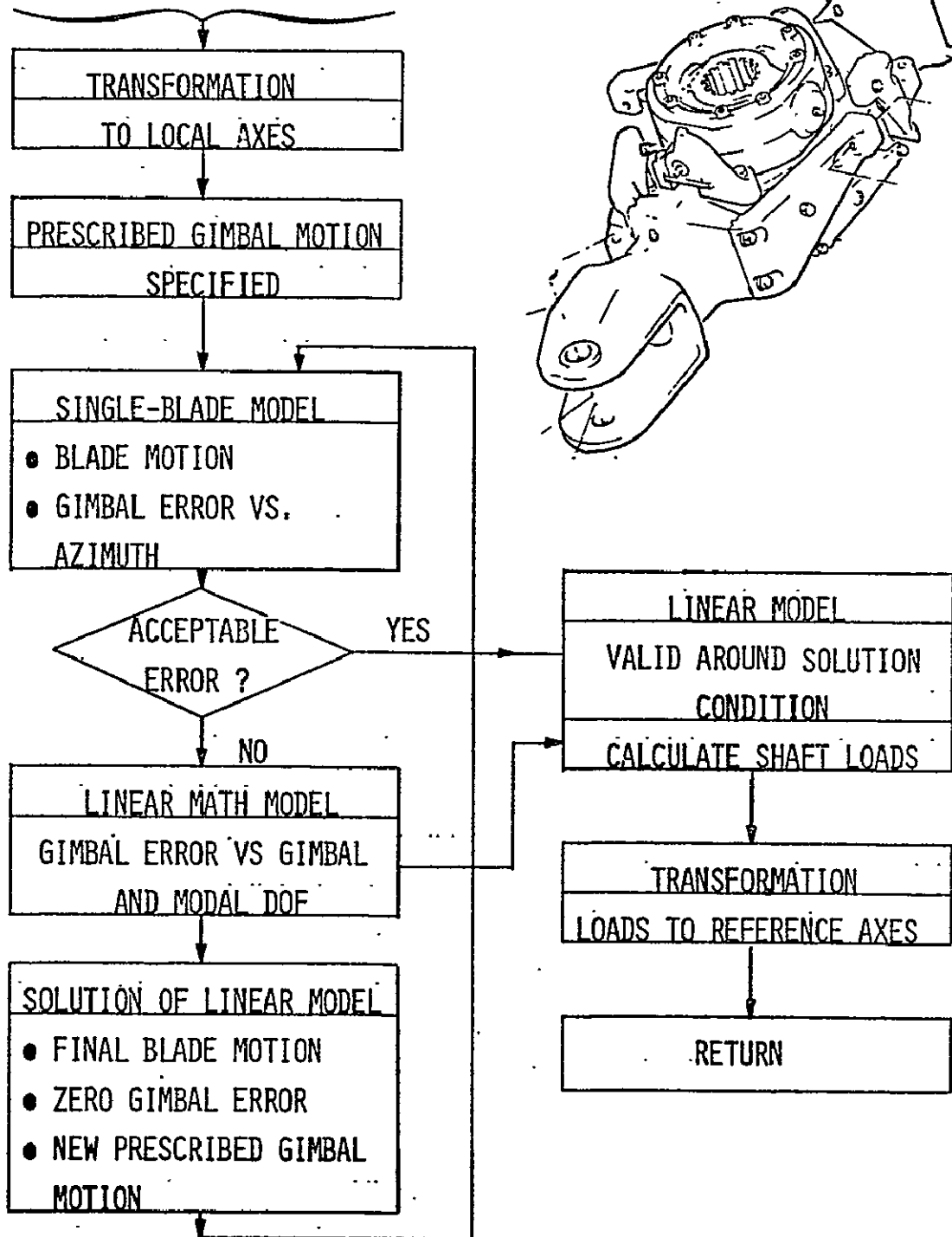
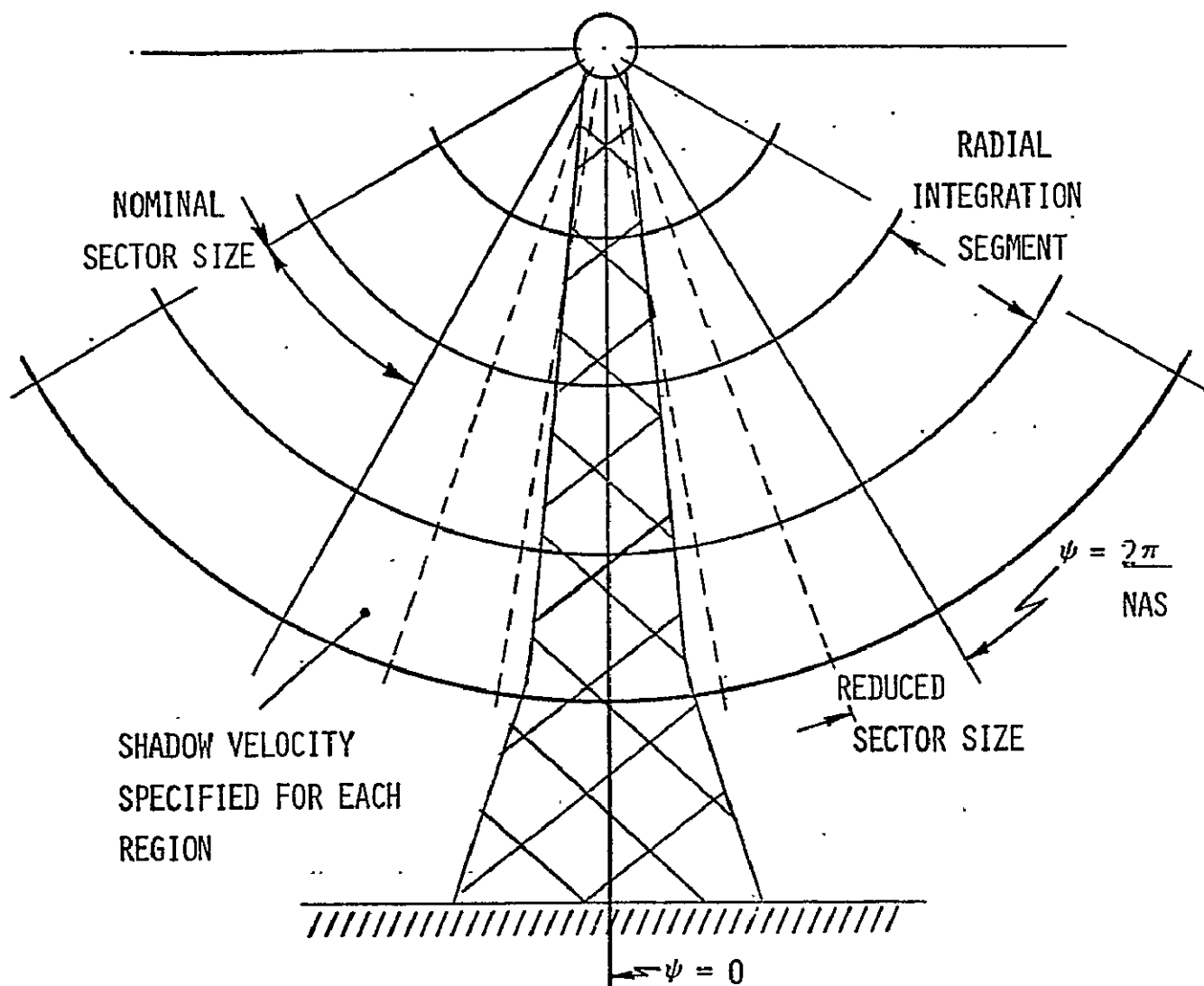


FIGURE 9. - ADVANCED SHADOW MODEL.



SHADOW PROFILE SPECIFIED AS FUNCTION
OF AZIMUTH AND RADIUS - KEYED TO
TOWER DRAG-ARBITRARY PROFILE

FIGURE 10.- MOSTAB OUTPUTS.

TRIM CONDITIONS

- CONTROLS
- LOADS
- MOTIONS
- WAKE

COMPREHENSIVE LOADS AND MOTIONS

- TIME AND FREQUENCY DOMAINS
- SIX DIRECTIONS AT ALL RADII

LINEAR MATH MODELS

- STABILITY AND CONTROL DERIVATIVES
 - OVERALL
 - INDIVIDUAL COMPONENTS
- ROLIMX DATA

FIGURE 11. - STEPS IN ROLIM PROCESS.

- A. ROLIMX PROCEDURES USE MOSTAB MODELS TO SYNTHESIZE LINEAR OPERATIONS FOR
- BLADE GENERALIZED FORCING FUNCTIONS
 - SHAFT LOADS
 - WAKE VELOCITIES
- AS FUNCTIONS OF
- BLADE MODAL COORDINATES (SINGLE BLADE)
 - SHAFT MOTIONS
 - CONTROLS
 - AIR VELOCITIES
- B. SINGLE-BLADE LINEAR MODEL EXPANDED TO FULL ROTOR - PHASE SHIFTING PROCEDURE
- C. ROTOR AND WAKE MODELS COMBINED WITH RIGID-BODY SHAFT EQUATIONS TO FORM ROLIM EQUATIONS
- D. ROLIM EQUATIONS TRANSFORMED TO MULTI-BLADE COORDINATES
- E. PERIODIC OPERATORS CONVERTED TO FREQUENCY DOMAIN

FIGURE 12. - THE ROTOR LINEAR MODELLING PROGRAM
ROLIM.

FINAL MODEL

$$M\ddot{Y} + B\dot{Y} + KY = Y_C C + Y_{\dot{C}} \dot{C} + Y_{\ddot{C}} \ddot{C} + Y_{\Omega} \Omega + Y_{\dot{\Omega}} \dot{\Omega}$$

$$Y = \left\{ \begin{array}{l} \text{SHAFT DOF} \\ \text{---} \\ \text{BLADE MODAL} \\ \text{DOF, ALL} \\ \text{MODES IN ALL} \\ \text{BLADES} \\ \text{---} \\ \text{OTHER AERO-} \\ \text{ELASTIC DOF} \end{array} \right\} \quad C = \left\{ \begin{array}{l} \text{CONTROLS} \end{array} \right\}$$

$\Omega, \dot{\Omega}$ ROTOR SPEED AND ACCELERATION . . .

PERIODIC OPERATORS PRESENTED AS TIME FUNCTIONS OR
SPECTRA - MODEL GENERATED IN SIX OPTIONAL CONFIG-
URATIONS, INCLUDING MULTI-BLADE COORDINATES

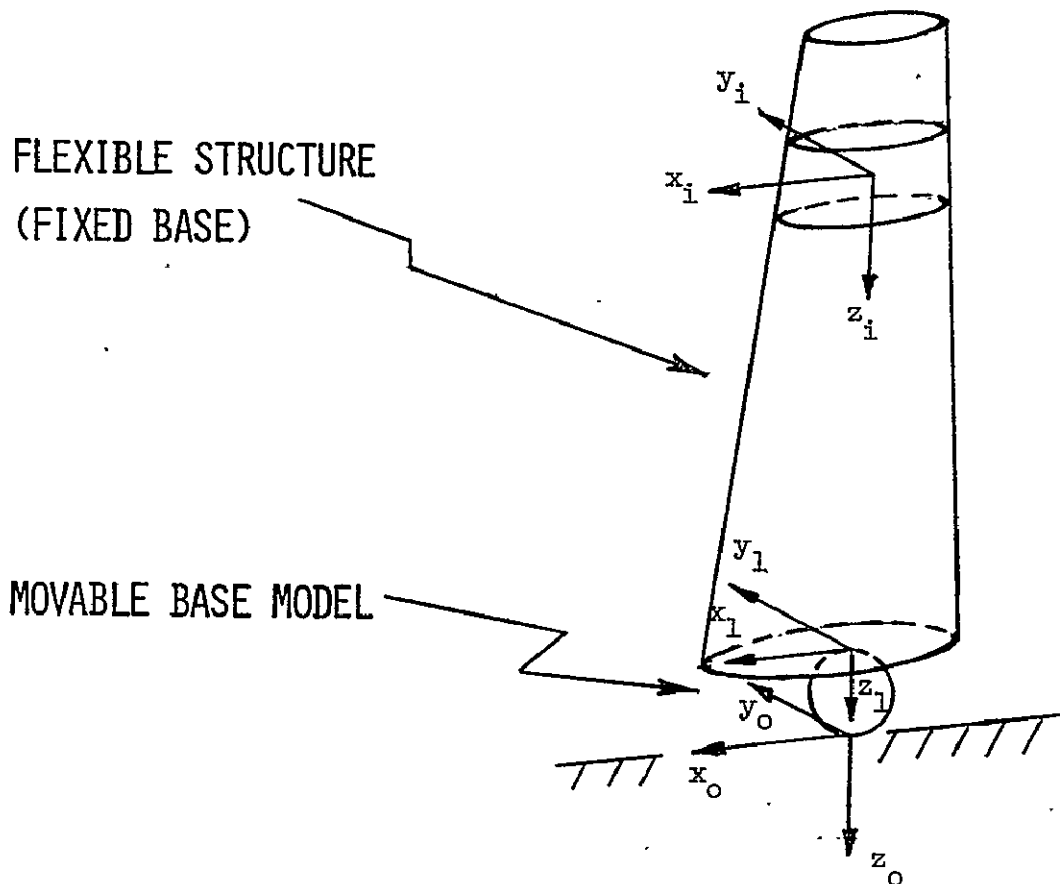
FIGURE 13. - EXAMPLE ROLIM PRINTOUTS.

X-WING AIRCRAFT HELD MODE SIMPLE AERO TEST CASE JULY 1976
ROTATING COORDINATE SYSTEM

PSI	OD(1, 1)	OD(2, 1)	OD(3, 1)	OD(4, 1)	OD(5, 1)	OD(6, 1)	OD(7, 1)	OD(8, 1)
0.0	-7.0433E-01	5.9183E-01	1.1603E-02	7.9126E-01	1.6856E+00	3.0459E+02	1.5851E-02	2.1147E-01
30.0	-3.3000E-01	8.6540E-01	-1.8242E-02	2.3717E+00	7.1785E-01	3.0437E+02	9.7300E-03	2.4656E-01
60.0	1.5152E-01	9.3080E-01	-1.4070E-02	2.2993E+00	-1.3305E+00	3.0457E+02	2.4499E-02	2.6370E-01
90.0	-7.0433E-01	5.9183E-01	1.1603E-02	7.9126E-01	1.6856E+00	3.0459E+02	2.3245E-02	2.7955E-01
120.0	-3.3000E-01	8.6540E-01	-1.8242E-02	2.3717E+00	7.1785E-01	3.0437E+02	1.2222E-02	2.7554E-01
150.0	1.5152E-01	9.3080E-01	-1.4070E-02	2.2993E+00	-1.3305E+00	3.0457E+02	1.2635E-02	2.6730E-01
180.0	-7.0433E-01	5.9183E-01	1.1603E-02	7.9126E-01	1.6856E+00	3.0459E+02	1.6150E-02	2.5867E-01
210.0	-3.3000E-01	8.6540E-01	-1.8242E-02	2.3717E+00	7.1785E-01	3.0437E+02	2.1440E-02	2.3652E-01
240.0	1.5152E-01	9.3080E-01	-1.4070E-02	2.2993E+00	-1.3305E+00	3.0457E+02	2.3375E-02	2.5744E-01
270.0	-7.0433E-01	5.9183E-01	1.1603E-02	7.9126E-01	1.6856E+00	3.0459E+02	2.5844E-02	2.9680E-01
300.0	-3.3000E-01	8.6540E-01	-1.8242E-02	2.3717E+00	7.1785E-01	3.0437E+02	3.9655E-02	2.5356E-01
330.0	1.5152E-01	9.3080E-01	-1.4070E-02	2.2993E+00	-1.3305E+00	3.0457E+02	3.9354E-02	1.9396E-01
PSI	OD(9, 1)	OD(10, 1)	OD(11, 1)	OD(12, 1)	OD(13, 1)	OD(14, 1)		
0.0	2.3245E-02	2.7955E-01	1.6150E-02	2.5867E-01	2.5644E-02	2.9680E-01		
30.0	1.2222E-02	2.7554E-01	2.1440E-02	2.3652E-01	3.9655E-02	2.5356E-01		
60.0	1.2635E-02	2.6730E-01	2.3375E-02	2.5744E-01	3.9354E-02	1.9396E-01		
90.0	1.6150E-02	2.5867E-01	2.5844E-02	2.9680E-01	1.5851E-02	2.1147E-01		
120.0	2.1440E-02	2.3652E-01	3.9655E-02	2.5356E-01	9.7300E-03	2.4656E-01		
150.0	2.3375E-02	2.5744E-01	3.9354E-02	1.9396E-01	2.4499E-02	2.6370E-01		
180.0	2.5844E-02	2.9680E-01	1.5851E-02	2.1147E-01	2.3245E-02	2.7955E-01		
210.0	3.9655E-02	2.5356E-01	9.7300E-03	2.4656E-01	1.2222E-02	2.7554E-01		
240.0	3.9354E-02	1.9396E-01	2.4499E-02	2.6370E-01	1.2635E-02	2.6730E-01		
270.0	1.5851E-02	2.1147E-01	2.3245E-02	2.7955E-01	1.6150E-02	2.5867E-01		
300.0	9.7300E-03	2.4656E-01	1.2222E-02	2.7554E-01	2.1440E-02	2.3652E-01		
330.0	2.4499E-02	2.6370E-01	1.2635E-02	2.6730E-01	2.3375E-02	2.5744E-01		

ORIGINAL PAGE IS
OF POOR QUALITY

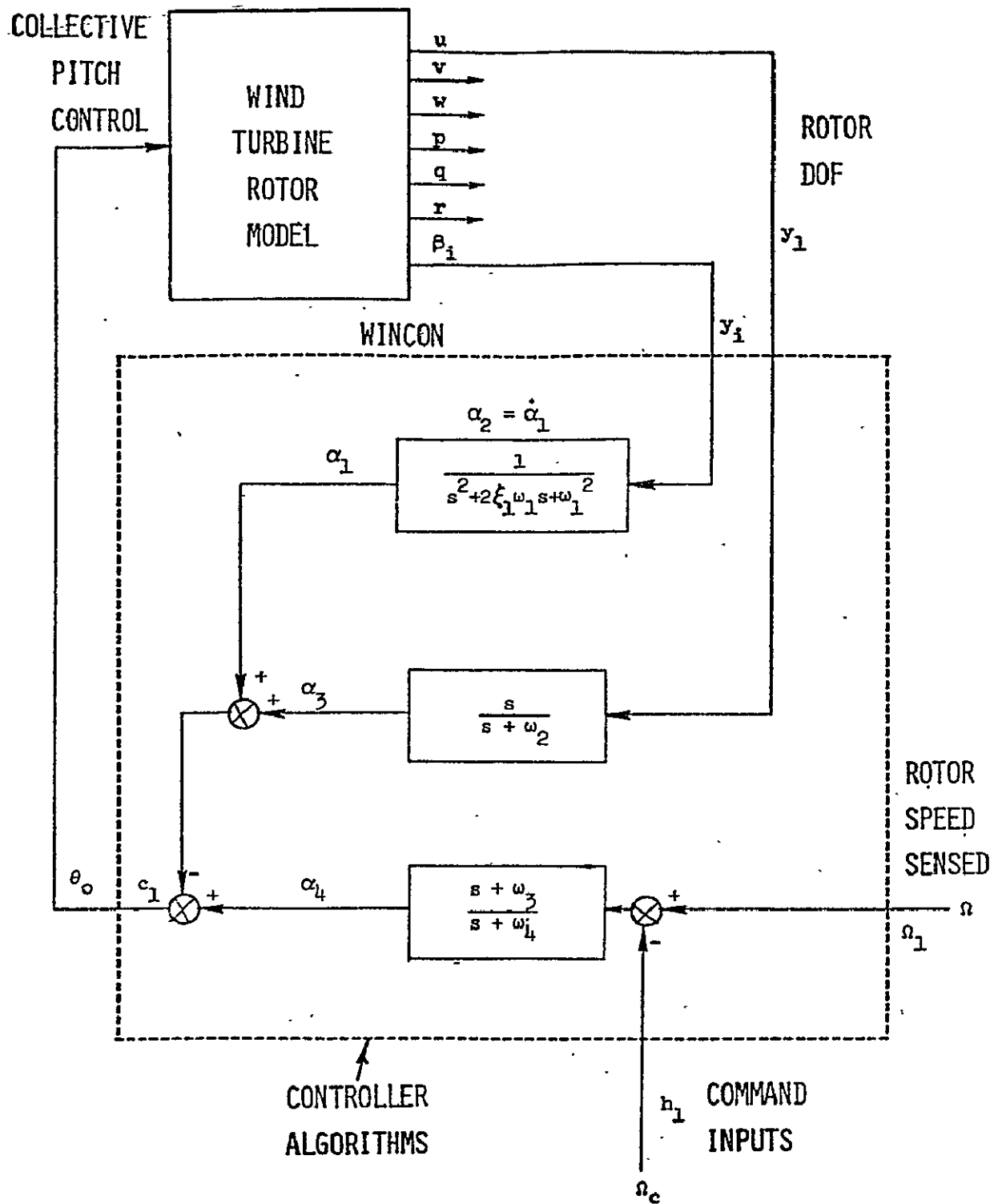
FIGURE 14. - TOWER MATH MODEL.



LINEAR TOWER MODEL: SUPERPOSITION OF

- MODAL MODEL OF TOWER MASS - ELASTIC STRUCTURE WITH FIXED BASE
- RIGID BODY MODEL ON ROTARY BASE

FIGURE 15. - SAMPLE CONTROL SYSTEM MODEL.



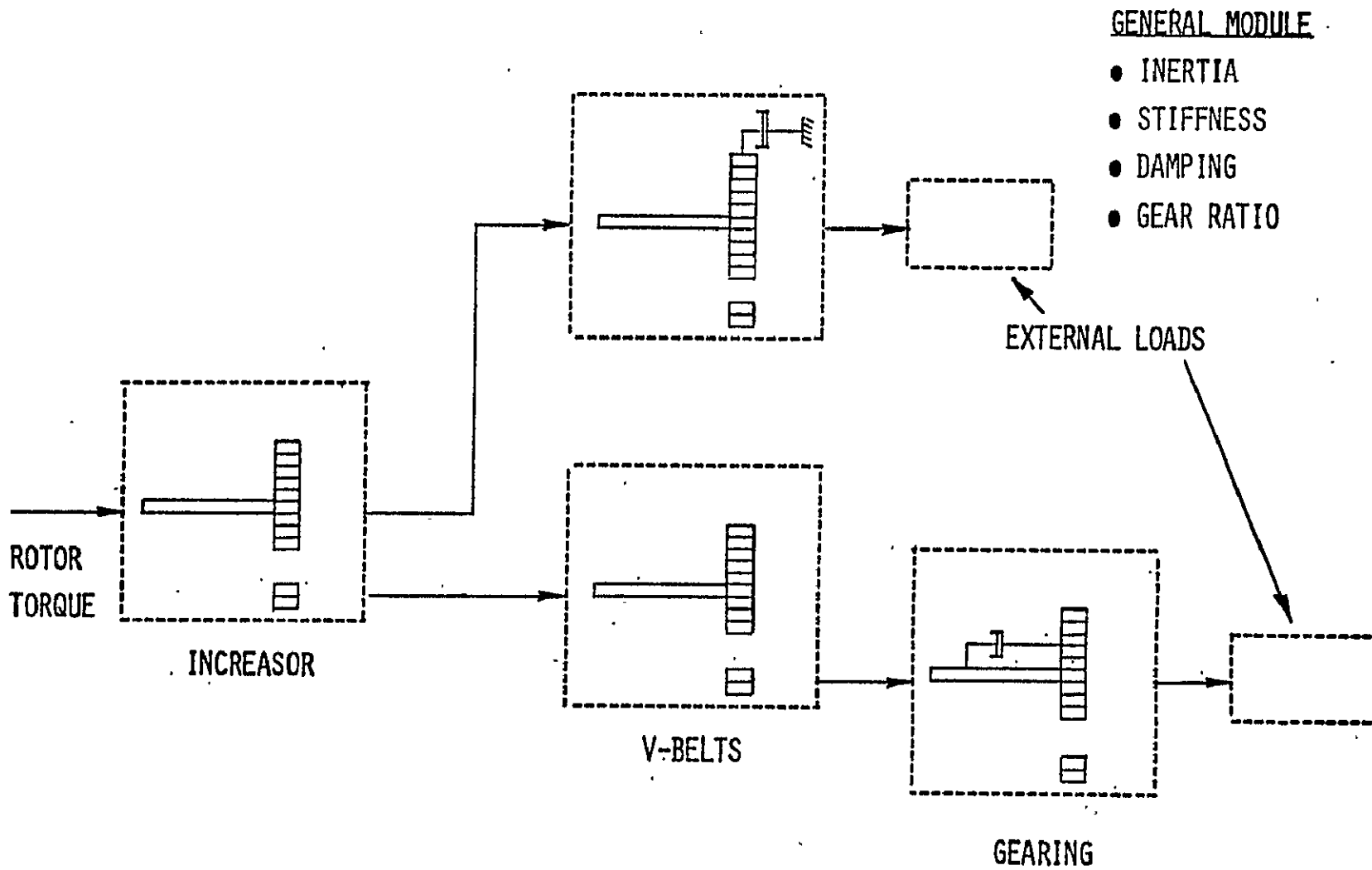
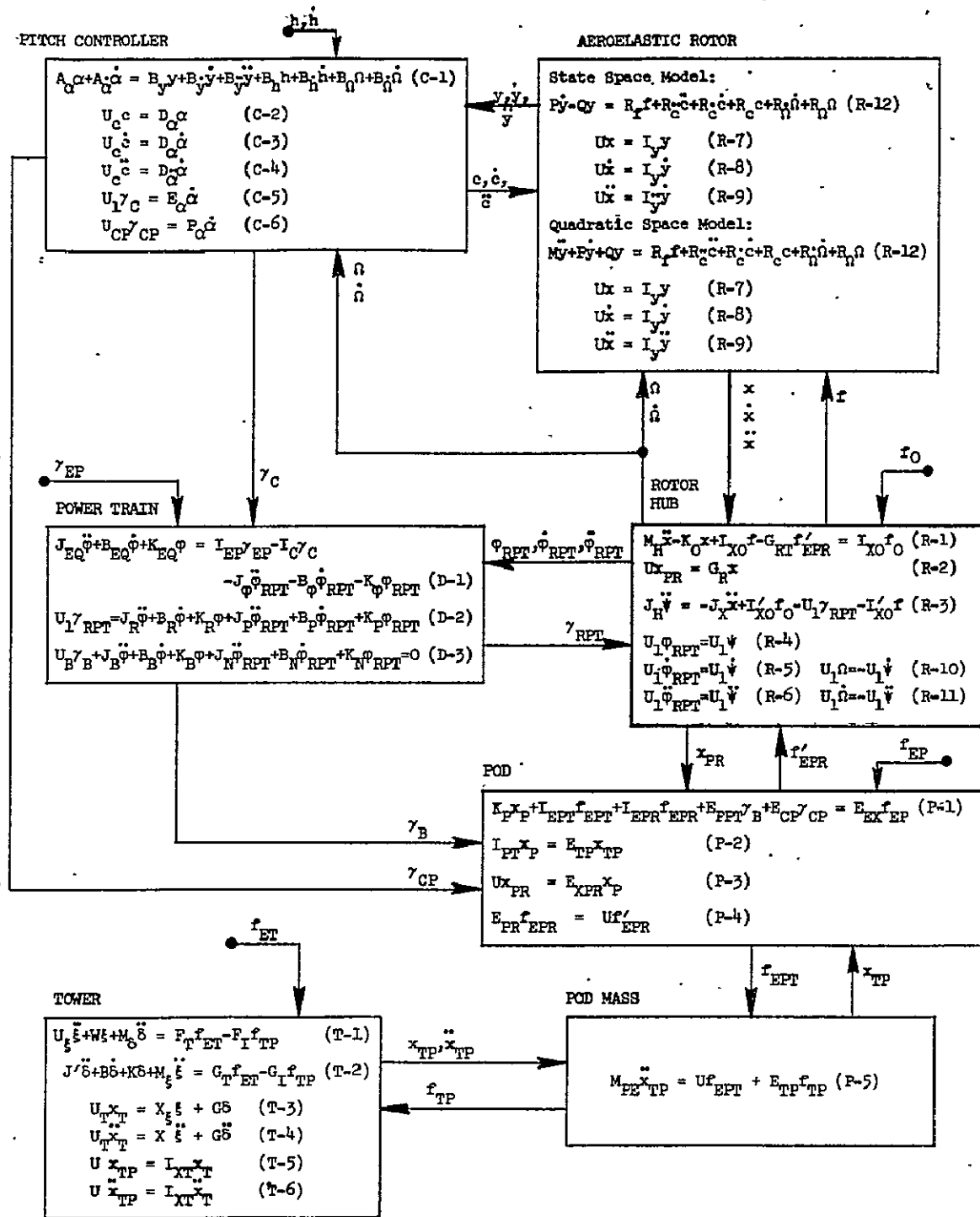


FIGURE 16. - POWER TRAIN DYNAMIC MATH MODEL.

FIGURE 17. WIND TURBINE SYSTEM BLOCK DIAGRAM.



ORIGINAL PAGE IS
OF POOR QUALITY

FIGURE 18. - LONG YOKE TEETERING DESIGN.

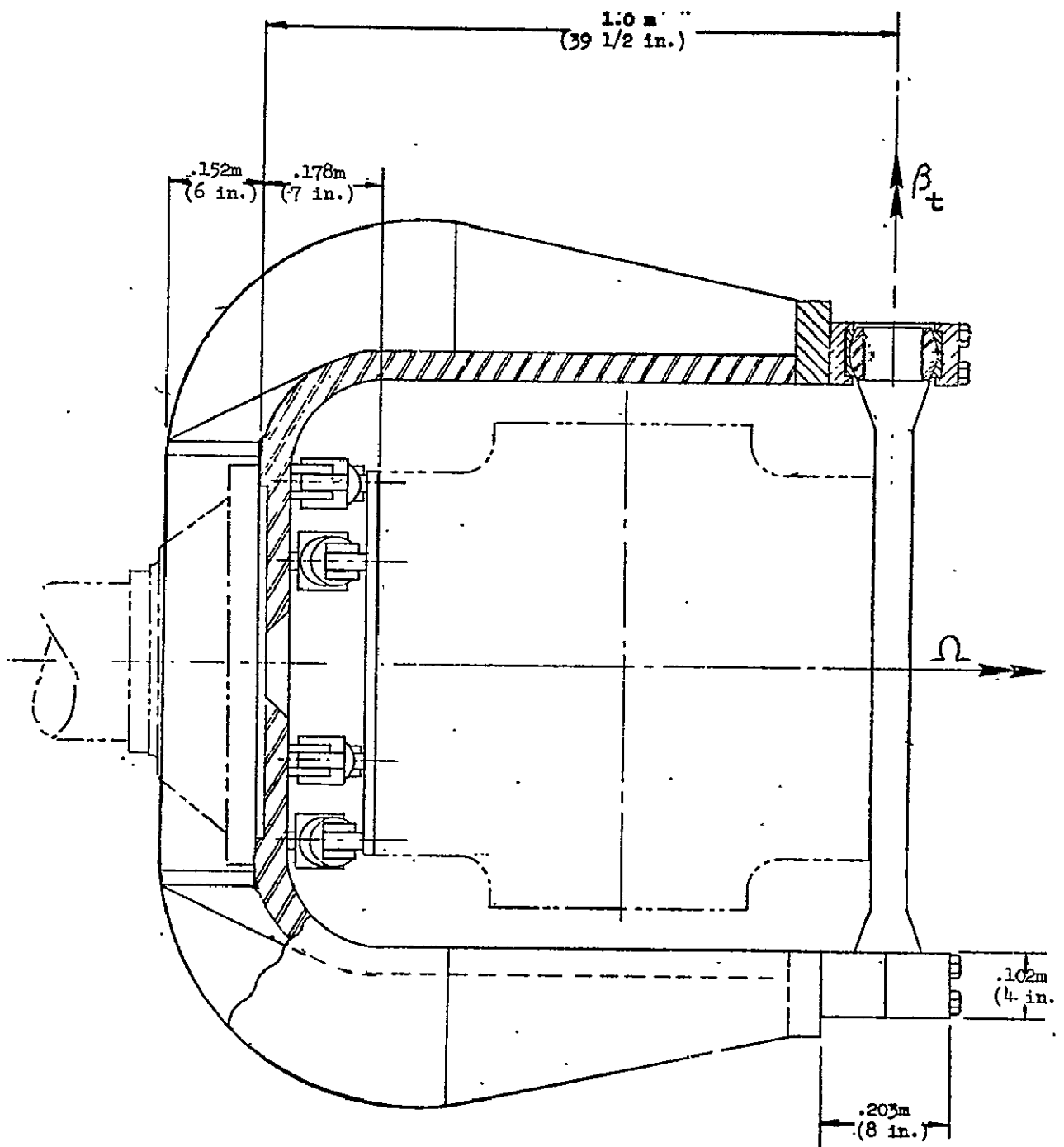


FIGURE 19. - SHORT YOKE TEETERING CONCEPT.

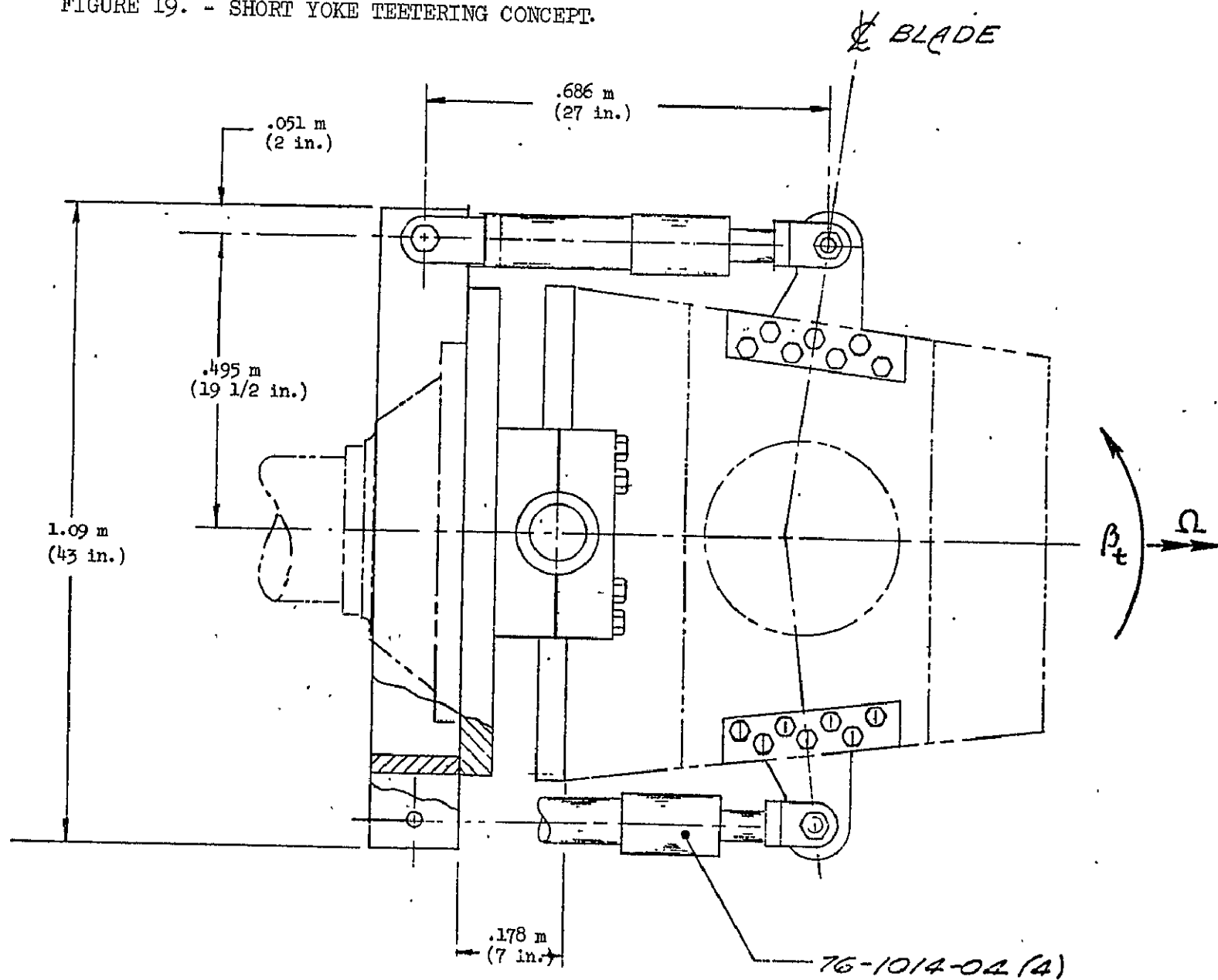


FIGURE 20. - LINKAGE TEETERING CONCEPT.

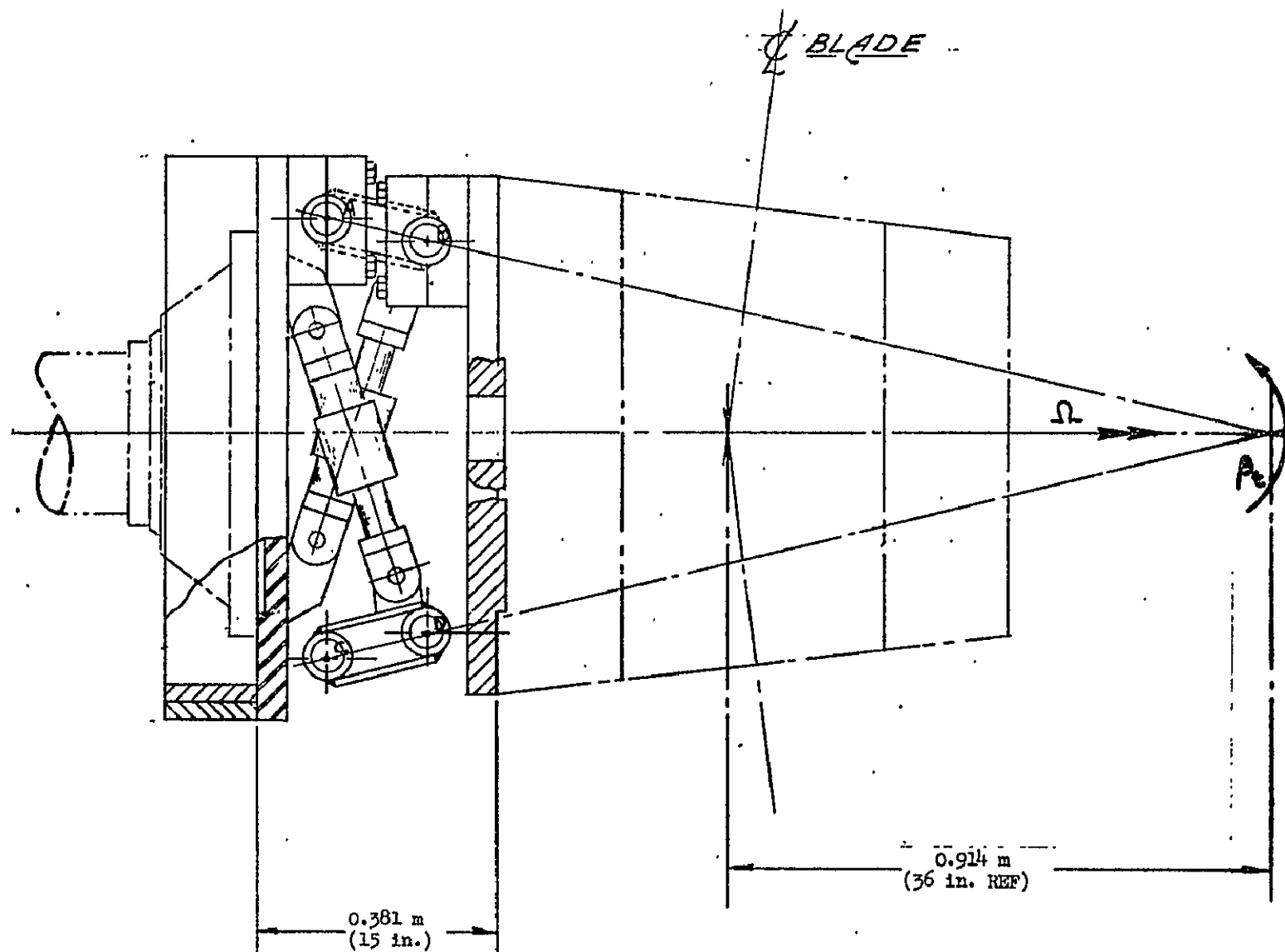


FIGURE 21. - ROOT OUT-OF-PLANE MOMENT.

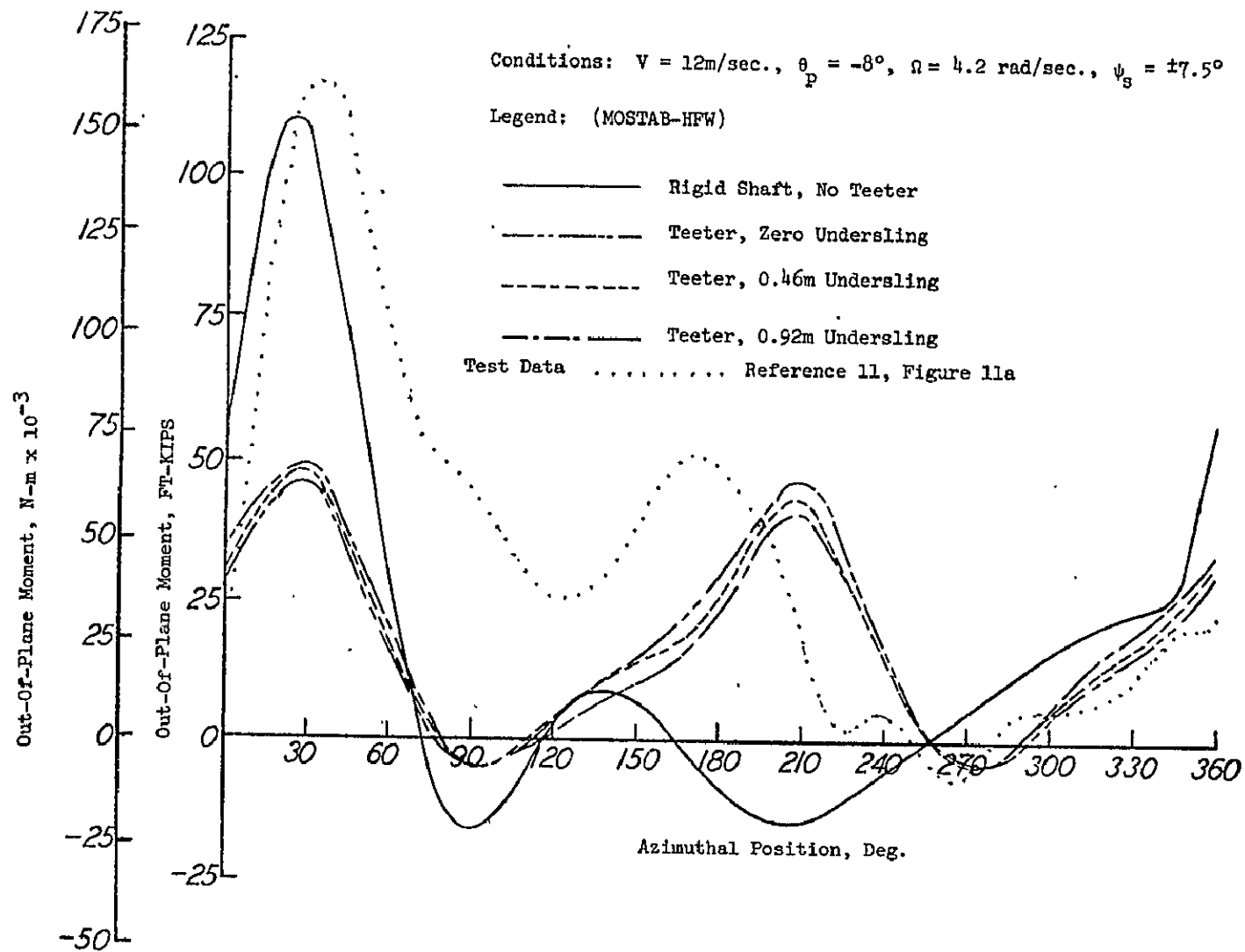


FIGURE 22. - ROOT IN-PLANE MOMENT.

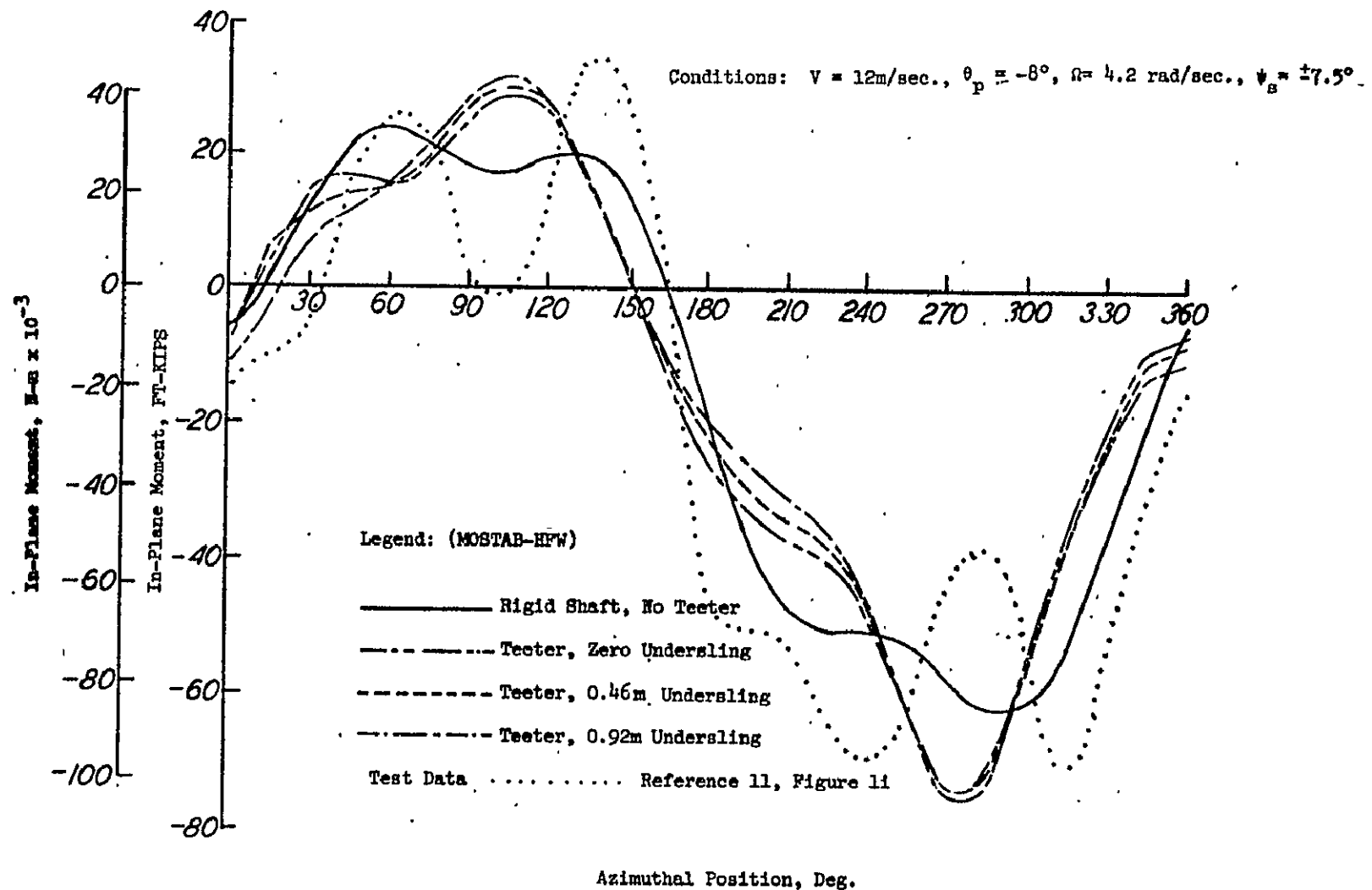


FIGURE 23. - BLADE TIP DEFLECTION.

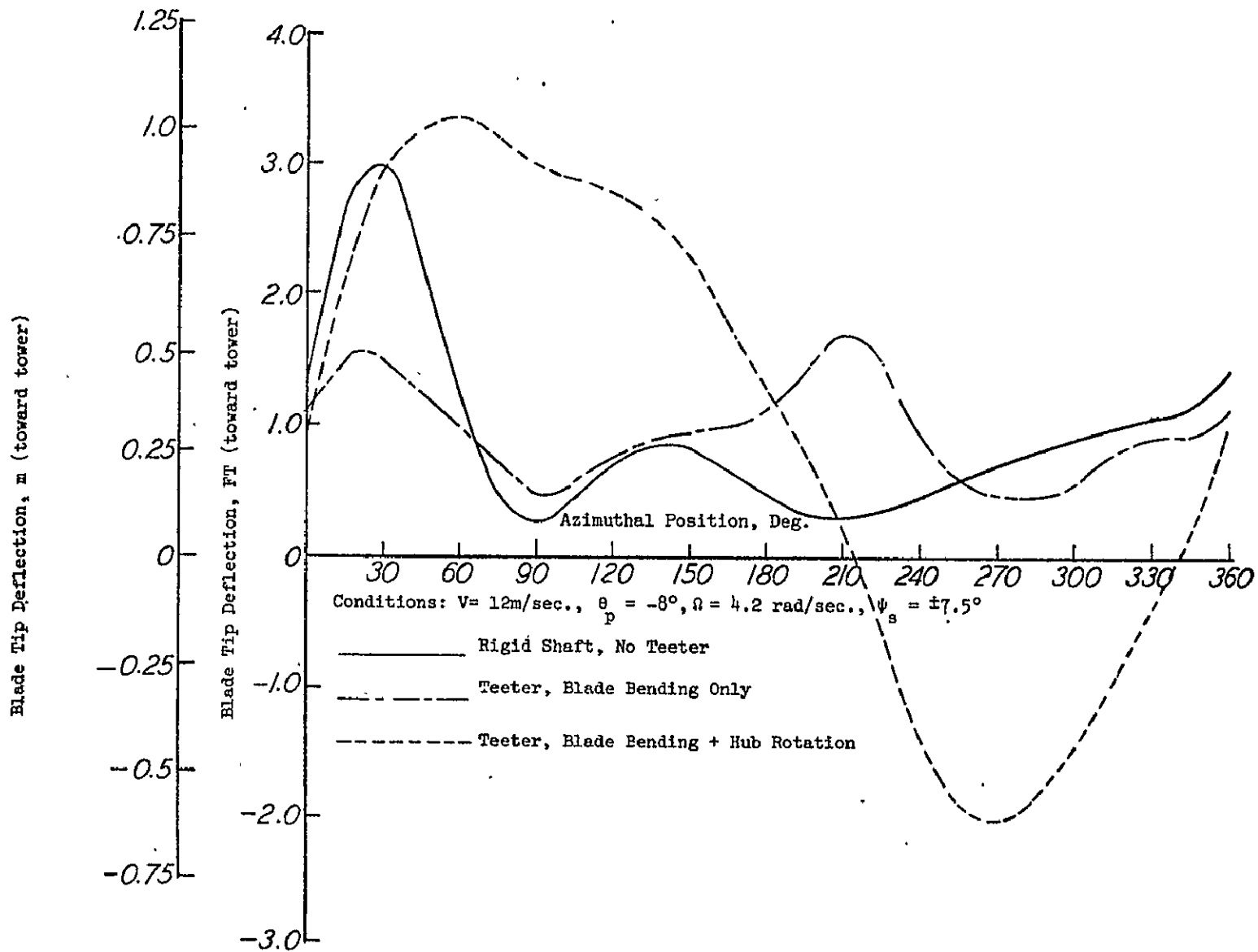
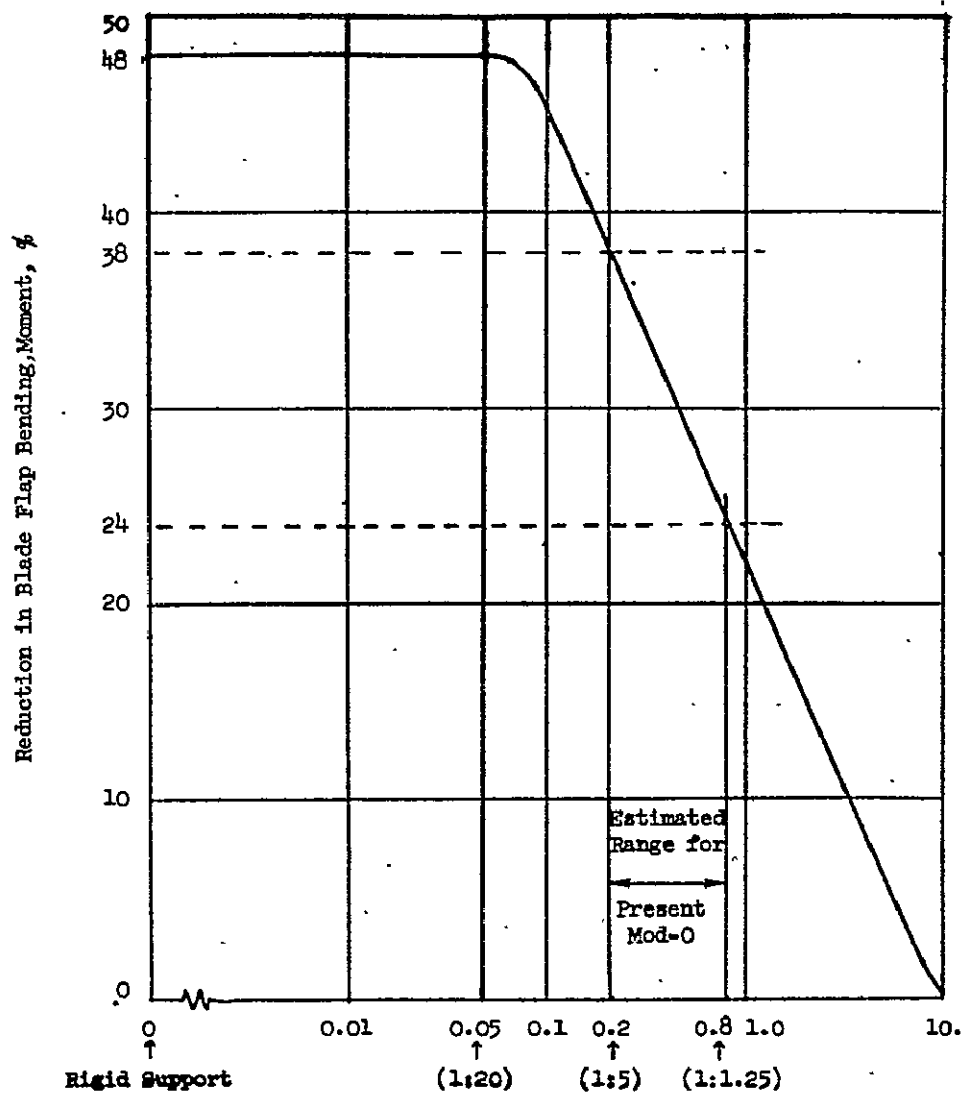
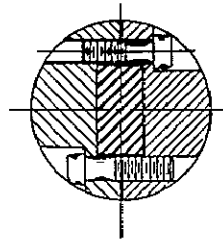


FIGURE 24. - BLADE MOMENT REDUCTION EXPECTED FROM TEETERING AS A FUNCTION OF PRESENT HUB SUPPORT STIFFNESS.

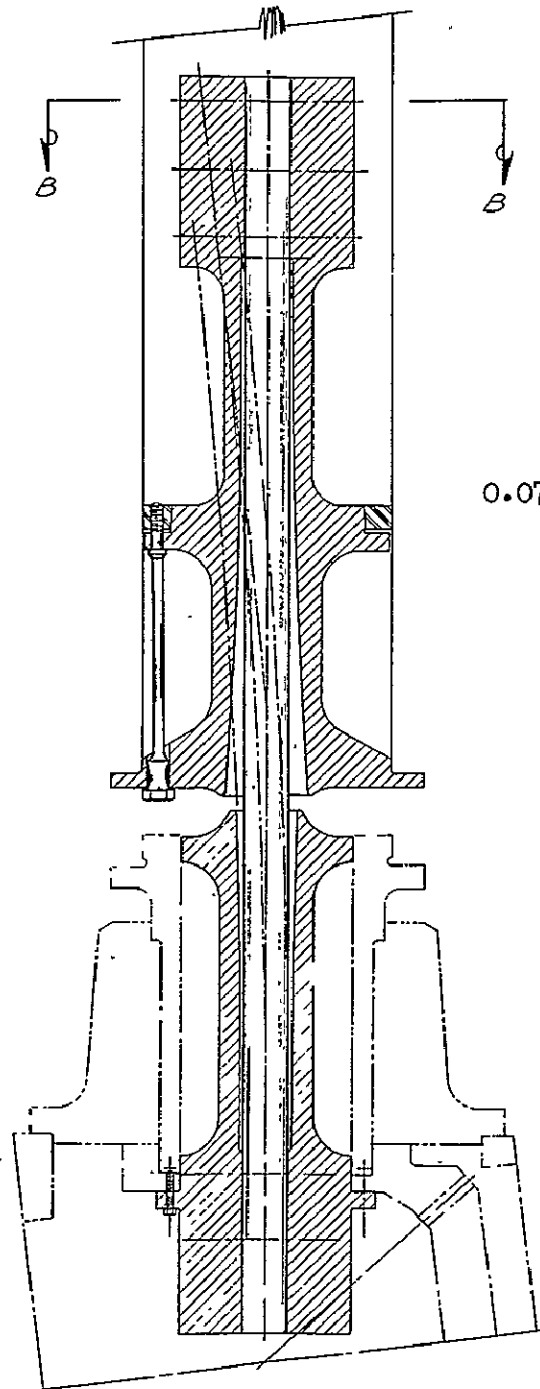


Present Ratio of Blade Stiffness to Hub Support Stiffness, $K_p/K_s (\omega_0)$



SECTION B-B

FIGURE 25. -
ELASTIC INTERFACE
FLEXURE A.



0.074m x 0.147m x 1.46m long

FLEXURE A

4340 STEEL H.T. 150,000-170,000
29" X 5.6" X 52.5" LONG

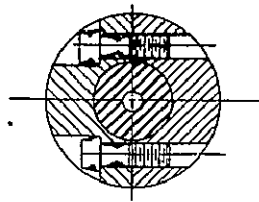
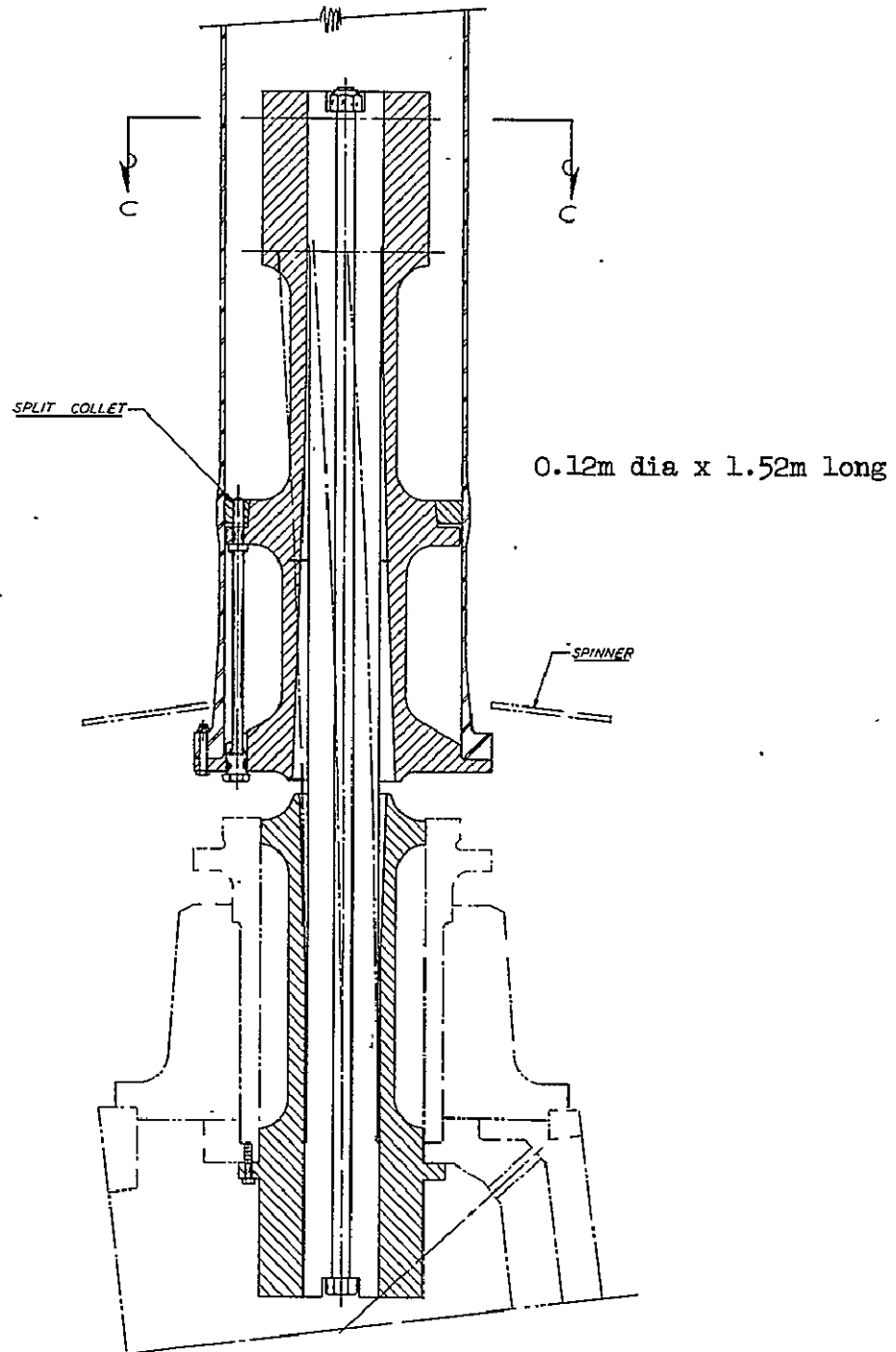


FIGURE 26. -
ELASTIC INTERFACE
FLEXURE B.

SECTION C-C



FLEXURE "B"

4340 STEEL H.T 150,000-170,000
4.73" DIA X 60" LONG

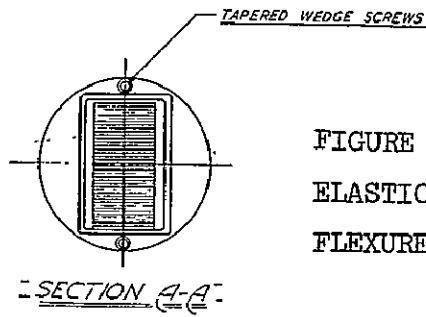
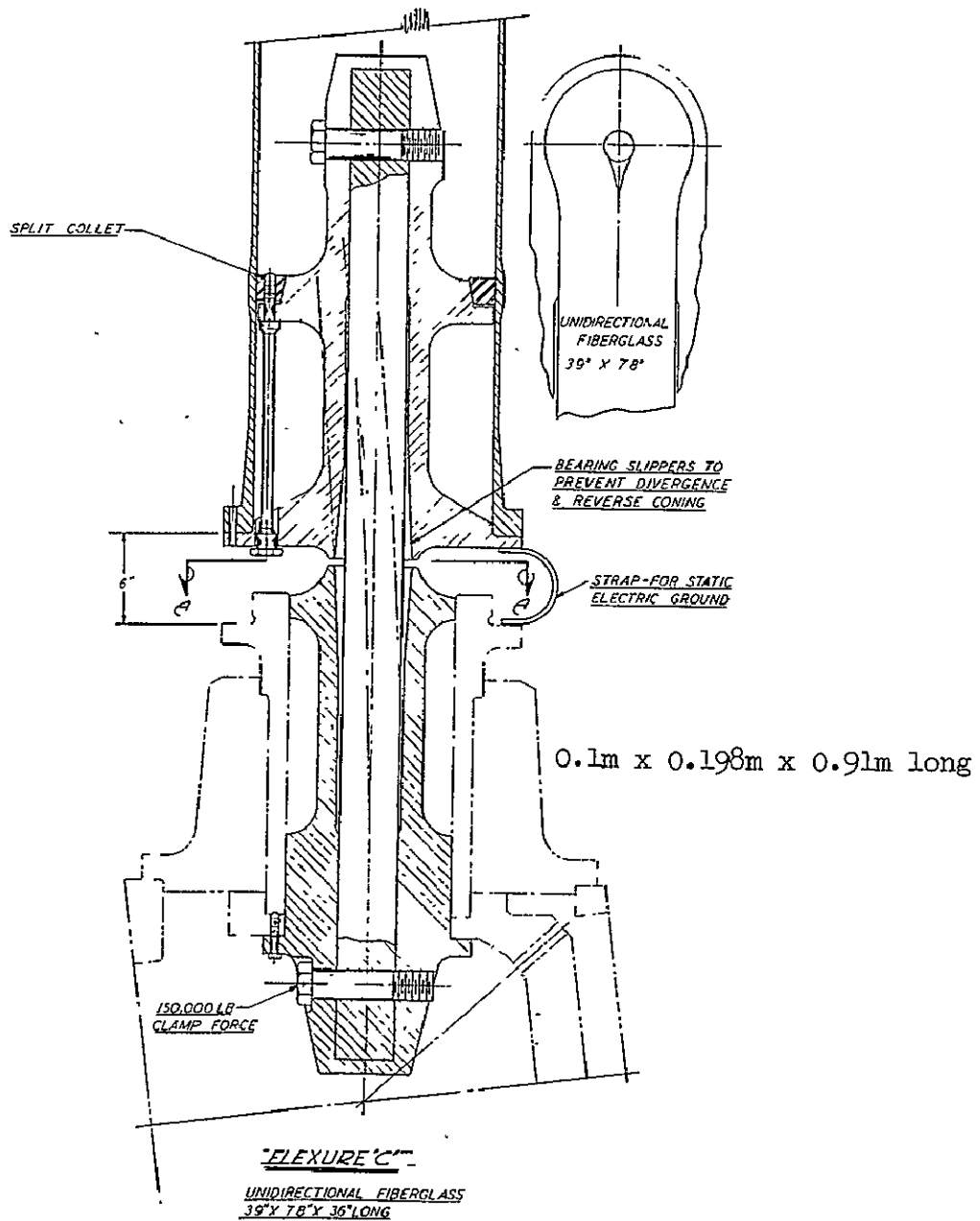
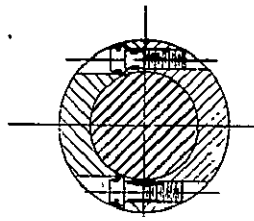


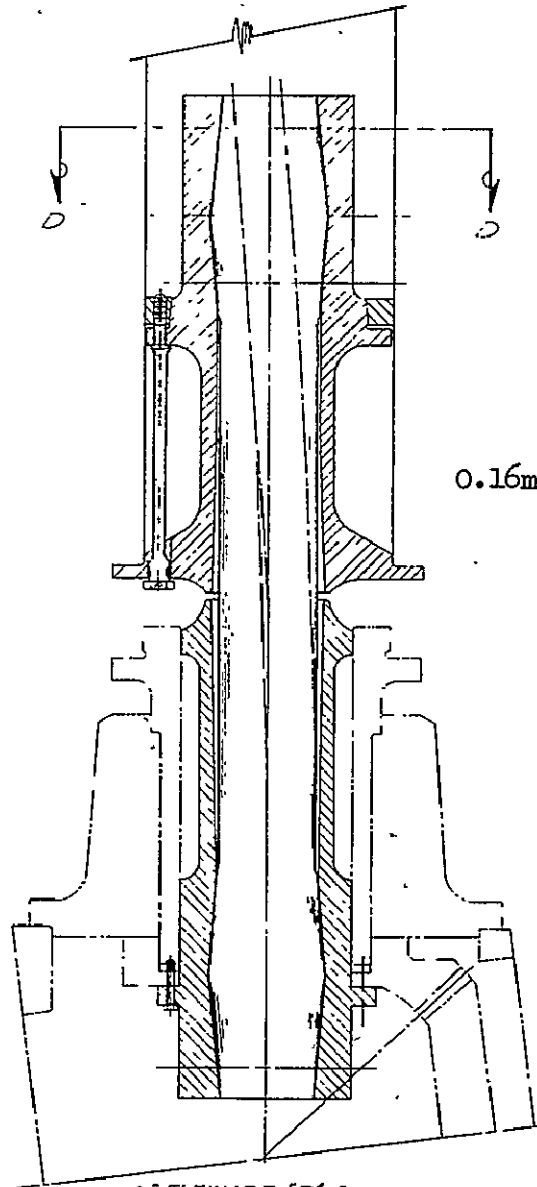
FIGURE 27. -
ELASTIC INTERFACE
FLEXURE C.





SECTION D-D

FIGURE 28. -
ELASTIC INTERFACE
FLEXURE D.



0.16m dia x 0.91m long

"FLEXURE D."
UNIDIRECTIONAL FIBERGLASS
6.30" DIA. X 36" LONG

FIGURE 29. - ROOT OUT-OF-PLANE BENDING MOMENT.

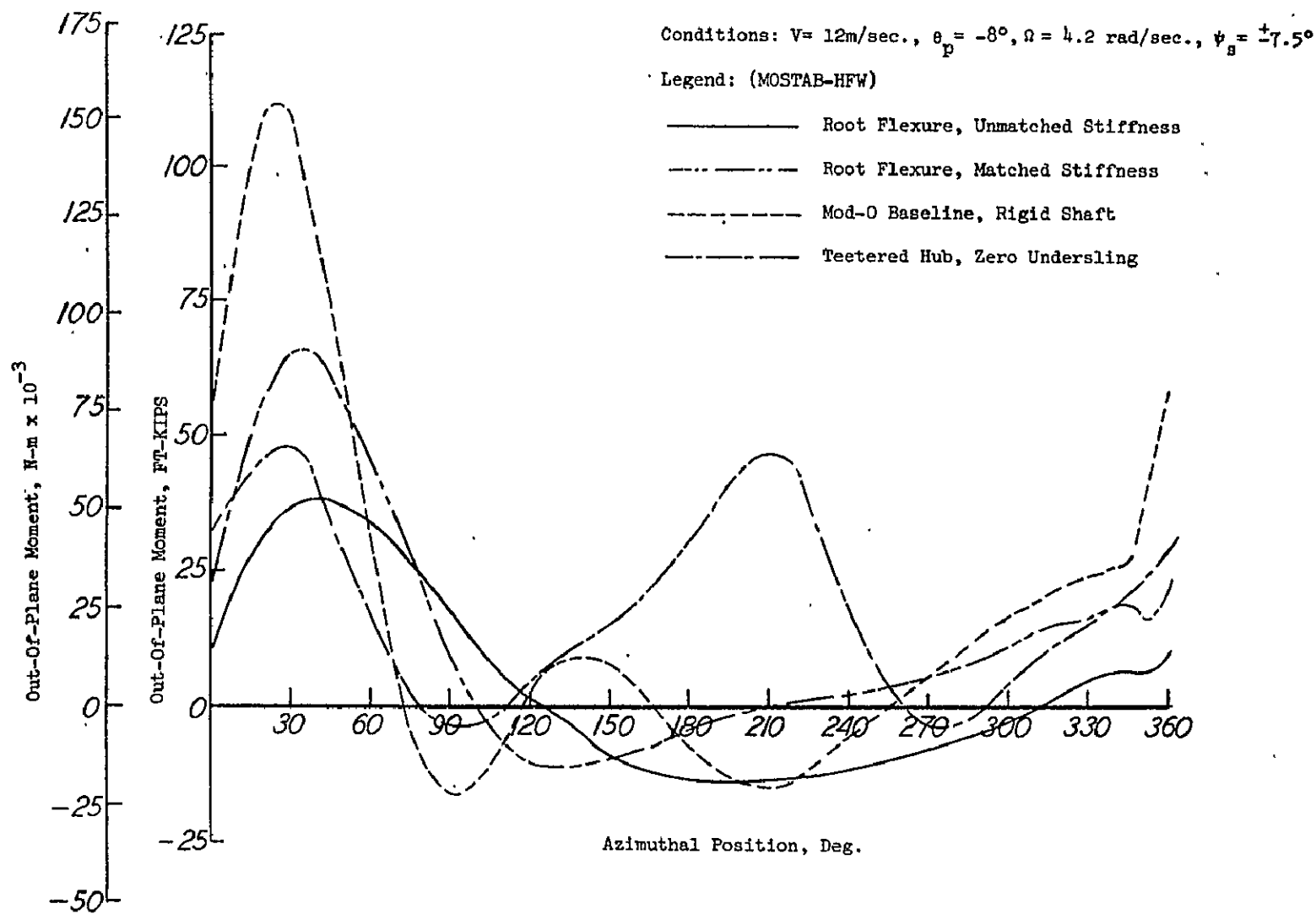


FIGURE 30. - ROOT IN-PLANE BENDING MOMENT.

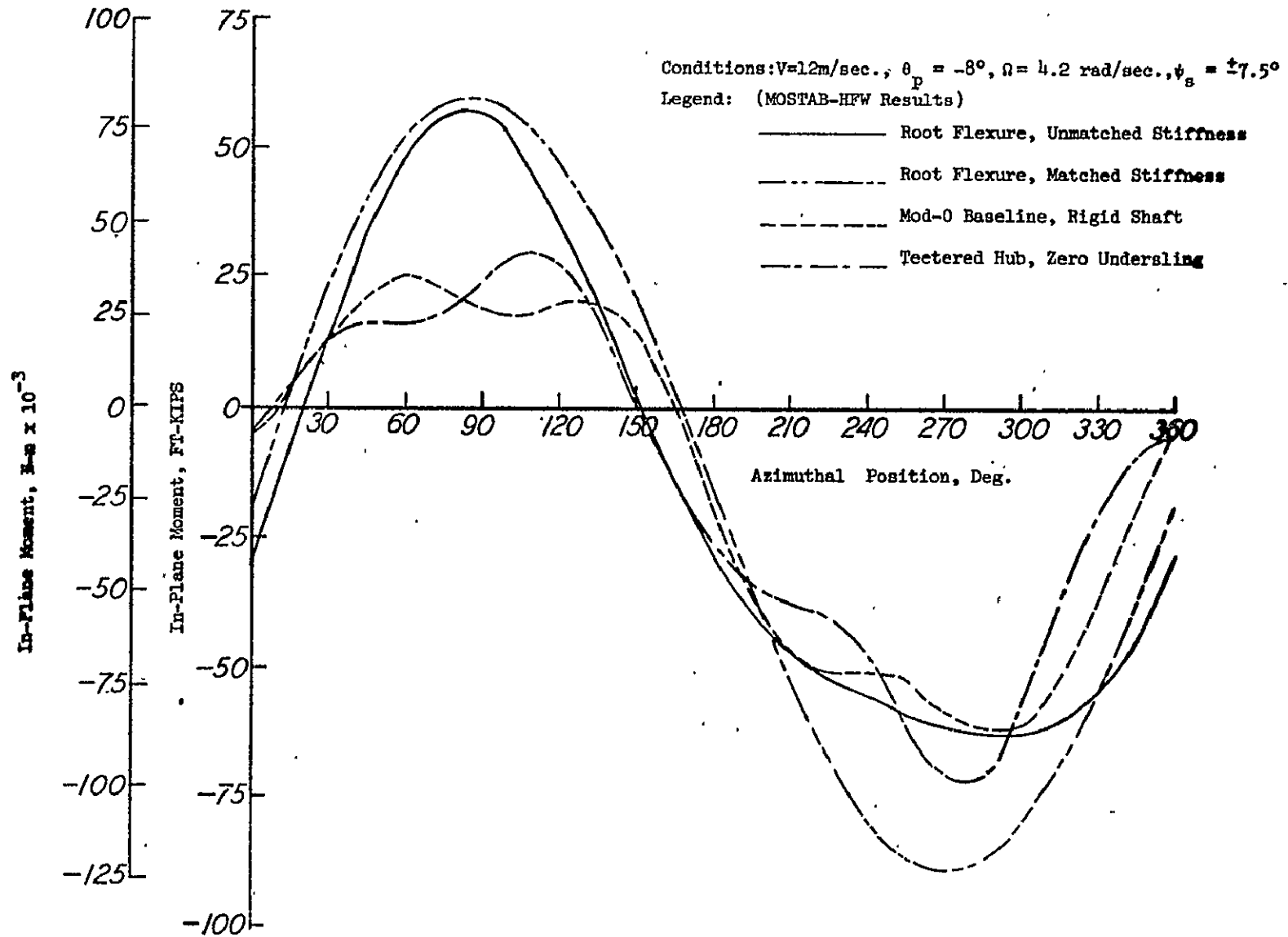


FIGURE 31. - BLADE TIP DEFLECTION.

